Epithelial-to-mesenchymal transition promotes immune escape by inducing CD70 in non-small cell lung cancer

Sandra Ortiz-Cuaran, Aurélie Swalduz, Jean-Philippe Foy, Solène Marteau, Anne-Pierre Morel, Frédérique Fauvet, Geneviève de Souza, Lucas Michon, Maxime Boussageon, Nicolas Gadot, et al.

Original Research Article

Epithelial-to-mesenchymal transition promotes immune escape by inducing CD70 in non-small cell lung cancer

Sandra Ortiz-Cuaran[1 ¥ *], Aurélie Swalduz[1,2 ¥], Jean-Philippe Foy[1], Solène Marteau[1], Anne-Pierre Morel[1], Frédérique Fauvet[1], Geneviève De Souza[1], Lucas Michon[1], Maxime Boussageon[1,2], Nicolas Gadot[5], Marion Godefroy[1], Sophie Léon[1], Antonin Tortereau[1], Nour-El-Houda Mourksi[1], Camille Leonce[1], Marie Alexandra Albaret[1], Anushka Dongre[3], Béatrice Vanbervliet[1], Marie Robert[1], Laurie Tonon[1], Roxane M Pommier[1], Véronique Hofman[4], Valéry Attignon[6], Sandrine Boyault, Carole Audoynaud[6], Jessie Auclair[6], Fanny Bouquet[7], Qing Wang[6], Christine Ménétrier-Caux[1], Maurice Pérol[2], Christophe Caux[1], Paul Hofman[4], Sylvie Lantuejoul[2,5], Alain Puisieux[1], Pierre Saintigny[1,2 *]

Authors' affiliations: 1. Univ Lyon, Claude Bernard Lyon 1 University, INSERM 1052, CNRS 5286, Centre Léon Bérard, Cancer Research Center of Lyon, Lyon, France. 2. Department of Medical Oncology, Centre Léon Bérard, Lyon, France. 3. Whitehead Institute for Biomedical Research, Cambridge, Massachusetts. 4. Laboratory of Clinical and Experimental Pathology, Université Côte d'Azur, CHU de Nice, University Hospital Federation OncoAge, Nice, France. 5. Research Pathology, Centre Léon Bérard, Lyon, France. 6. Genomics Platform, Centre Léon Bérard, Lyon, France. 7. Institute Roche, France.

¥ These authors contributed equally to this work.

*** Corresponding authors:**

Sandra Ortiz-Cuaran, Univ Lyon, Claude Bernard Lyon 1 University, INSERM 1052, CNRS 5286, Centre Léon Bérard, Cancer Research Center of Lyon. 28 rue Laennec, 69373 Lyon Cedex 08, France; Tel: +33(0)469856199; email: sandra.ortiz-cuaran@lyon.unicancer.fr

Pierre Saintigny, Univ Lyon, Claude Bernard Lyon 1 University, INSERM 1052, CNRS 5286, Centre Léon Bérard, Cancer Research Center of Lyon and Department of Medical Oncology, Centre Léon Bérard; 28 rue Laennec, 69373 Lyon Cedex 08, France; Tel: +33-(0)469856097; Fax: +33-(0)478782868; email: Pierre.SAINTIGNY@lyon.unicancer.fr

Keywords: CD70, lung cancer, epithelial-to-mesenchymal transition, sarcomatoid carcinomas

Running title: CD70 and immune evasion in mesenchymal lung cancers.

CONFLICTS OF INTEREST

SO-C: None. AS: Honoraria for Advisory Boards: Roche, Bristol-Myers Squibb, Takeda Symposiums: Roche, AstraZeneca, Boehringer-Ingelheim, Bristol-Myers Squibb, Pfizer, Takeda. JPF: None. SM: None. APM: None. FF: None. MB: None. AD: None. CL: None. MR: None. NM: None. LM: None. MG: None. SL: None. AT: None. LT: None. SB: None. RMP: None. MAA: None. GDS: None. VH: None. NG: None. VA: None. CA: None. JA: None. FB: Current employee at F. Hoffman La Roche. CMC: None. QW: None. MP: None. CC: None. PH: None. SL: consultant fees from MSD, BMS, Astra Zeneca, Abbvie, Bayer, Takeda. AP: None. PS: Research funding from Astra-Zeneca, Roche, Genentech, BMS, Novartis and HTG Molecular Diagnostics. Scientific Advisory Board member of HTG Molecular Diagnostics

HIGHLIGHTS

- The EMT-inducer ZEB1 modulates the expression of CD70, a regulatory ligand from the tumor necrosis factor ligand family.
- CD70 expression is enriched in pulmonary sarcomatoid carcinomas, a rare lung cancer subtype that is often associated with poor prognosis and resistance to systemic therapies.
- In pulmonary sarcomatoid carcinomas, CD70 expression is associated with the acquisition of features of an immunosuppressive environment.

ABSTRACT

Introduction: Epithelial-to-mesenchymal transition (EMT) is associated with tumor aggressiveness, drug resistance and poor survival in non-small cell lung cancer (NSCLC) and other cancers. The identification of immune-checkpoint ligands (ICPLs) associated with NSCLCs that display a mesenchymal phenotype (mNSCLC), could help defining subgroups of patients who may benefit from treatment strategies using immunotherapy.

Methods: We evaluated ICPL expression *in silico* in 130 NSCLC cell lines. *In vitro*, CRISPR/Cas9-mediated knockdown and lentiviral expression were used to assess the impact of ZEB1 expression on CD70. Gene expression profiles of lung cancer samples from the TCGA (n=1,018) and a dataset from MD Anderson Cancer Center (n=275) were analyzed. Independent validation was performed by immunohistochemistry and targeted-RNA sequencing in 154 NSCLC whole sections, including a large cohort of pulmonary sarcomatoid carcinomas (SC, n=55).

Results: We uncover that expression of CD70, a regulatory ligand from the tumor necrosis factor ligand family, is enriched in mNSCLC *in vitro* models. Mechanistically, the EMT-inducer ZEB1 impacted *CD70* expression and fostered increased activity of the *CD70* promoter. CD70 overexpression was also evidenced in mNSCLC patient tumor samples and was particularly enriched in SC, a lung cancer subtype associated with poor prognosis. In these tumors, CD70 expression was associated with decreased $CD3^+$ and $CD8^+$ T-cell infiltration and increased T-cell exhaustion markers.

Conclusion: Our results provide evidence on the pivotal roles of CD70 and ZEB1 in immune-escape in mNSCLC, suggesting that EMT might promote cancer progression and metastasis not only by increasing cancer cell plasticity, but also by reprogramming the immune response in the local tumor microenvironment.

INTRODUCTION

Recent advances in the modulation of immune checkpoints (ICPs) or their ligands (ICPLs) have resulted in durable tumor regressions in different cancer types[1–5]. In non-small cell lung cancer (NSCLC), therapeutic blockade of programmed cell death 1 (PD-1), programmed death ligand-1 (PD-L1), and cytotoxic T lymphocyte–associated protein 4 (CTLA-4) have demonstrated clinically meaningful antitumor activity in cases that do not harbor a targetable genomic alteration, even in heavily pre-treated patients.

Epithelial-to-mesenchymal transition (EMT) is a fundamental embryonic process during which polarized epithelial cells acquire a more spindle-like mesenchymal morphology. This process is associated with increased cancer cell plasticity, invasiveness, resistance to therapy and poor prognosis in multiple cancers, including NSCLC [6–9]. Generally, NSCLC displaying a mesenchymal phenotype (mNSCLC) are associated with an immunosuppressive microenvironment characterized by deregulated expression of immunoproteasome subunits, intratumoral $CD8^+$ T-cell suppression (*i.e.* through the regulation of PD-L1) and higher levels of tumor infiltration by $CD4^+FOXP3^+$ regulatory T cells (Tregs) [10–13].

Activation of EMT is orchestrated by a network of EMT-inducing transcription factors (EMT-TFs) that interact with epigenetic regulators to control the expression of proteins involved in cell polarity, cell–cell contact, cytoskeleton structure and extracellular matrix degradation[14]. The Zinc-finger E-box-binding Homeobox-1 (ZEB1) is a transcription factor that promotes EMT. Indeed, ZEB1-induced EMT is a critical event in lung cancer progression [15] and is also implicated in the regulation of the microRNA-200-dependent expression of PD-L1 on lung cancer cells [13].

CD70 is a type-II transmembrane glycoprotein that functions as the regulatory ligand of CD27, a costimulatory receptor of the tumor necrosis factor (TNF) superfamily. CD70 is expressed on activated immune cells, including a broad range of T cells (naïve, αβ, γδ, and memory T cells), B cells, dendritic cells and NK cells [16,17]. Interestingly, aberrant CD70 expression has

been described in solid tumors and lymphomas and is reported to induce local immune-suppression in glioblastoma and renal cell carcinoma[16,18].

Here, we demonstrate that modulation of *ZEB1* impacts the expression of CD70 in mesenchymal *in vitro* models of NSCLC. Further, we provide evidence that CD70 is upregulated in mNSCLC patient samples and is associated with an immunosuppressive tumor microenvironment. This finding is of particular importance in pulmonary sarcomatoid carcinomas, a lung cancer subtype with mesenchymal morphology, that is often associated with poor prognosis and resistance to chemotherapy [19,20], and that currently represents a relevant clinical challenge. Overall, our results highlight a novel concept that might have a direct impact on the development and use of immunotherapeutic strategies for EMT-driven tumors.

METHODS

In silico analysis

Five independent datasets of NSCLC or human bronchial epithelial cell lines, with available gene expression data, were mined from public databases. Four sets were downloaded from Gene Expression Omnibus: 1- a set of 130 NSCLC cell lines included in the Cancer Cell Line Encyclopedia (GSE36133); 2- a set of 112 NSCLC and 30 immortalized human bronchial epithelial cells (HBEC); 3- a set of 275 lung tumors (GSE41271) including 183 lung adenocarcinomas (ADC), 80 lung squamous-cell carcinomas (SqCC), 4 pulmonary sarcomatoid carcinomas (SC) and 8 other lung tumors (3 large cell carcinomas, 2 adenosquamous, 1 with both small-cell and non-small-cell subtypes and 1 undifferentiated); and 4- a set of a HBEC genetically manipulated to overexpress ZEB1 ($HBEC^{ZEB1}$) and its corresponding isogenic cells ($HBEC^{pMSCV}$) (GSE77925). Gene expression profiles of 517 lung ADC as well as 501 lung SqCC were downloaded from the Cancer Genome Atlas (TCGA) using the TCGA2STAT R package. Normalization of each dataset is described in Supplementary Methods.

Western-blot analysis

Cells from subconfluent cultures were lysed and proteins were extracted by Laemmli lysis buffer. Antibodies included mouse monoclonal E-Cadherin clone 36 (1:1000) from BD Biosciences (San Jose, CA, USA), mouse monoclonal anti-vimentin clone v9 (1:500) from Dako-Agilent, (Carpinteria, CA, USA), rabbit polyclonal anti-ZEB1 clone H-102 (1:500) from Santa-Cruz Biotechnology(Dallas, TX, USA), mouse monoclonal anti-TWIST1 clone TWIST2C1a (1:50), rabbit monoclonal anti-actin clone EPR16769 (1:5000) and rabbit polyclonal anti-SNAIL+SLUG (1:1000) all from Abcam (Cambridge, UK) and anti-mouse and anti-rabbit HRP-secondary antibodies (1:3000) from Cell Signaling Technology. Actin immunostaining was revealed by ECL (Amersham) and the other protein immunostaining by ECL Clarity (Amersham).

Gene reporter assays

$2x10^6$ HEK293T cells were transfected by calcium phosphate precipitation with total lentiviral expression vectors (pCMVdeltaR8.91, phCMVG-VSVG and HPRM39432-LvPG04). The pEZX-LvPG04 contains the *Gaussia* luciferase reporter gene under control of the CD70 promoter (promoter Length: 1497 bp; sequence length upstream of TSS: 1363 bp; sequence length downstream of TSS: 133 bp) and SeAP as an internal control. Forty-eight hours after transfection, the supernatant was collected, filtered, supplemented with 5µg/ml polybrene (Sigma) and combined with 200,000 target cells (PC9 empty vector or PC9 ZEB1 expressing cells) for 5 h. At 72 h after infection, cells were treated with doxycycline (Sigma) was added in the cell medium at concentration of 1µg/ml for 48 h, supernatants were collected and subjected to the Secrete-Pair Dual Luminescence Assay (GeneCopoeia), according to the manufacturer's instructions.

CRISPR/Cas 9 assay

Cells transduction. HCC44 cells were infected with an all-in-one lentivirus expressing in the same plasmid the nuclease Cas9 and the sgRNA ZEB1. One target against ZEB1 gene was

used for this nuclease system. To produce all-in-one sgRNA ZEB1 or control lentiviral particles, $2x10^6$ HEK293T cells were transfected by Genejuice precipitation with 13.02µg of total lentiviral expression vectors [5.1µg of pCMVdeltaR8.91, 1.32µg phCMVG-VSVG and 6.6µg pLenti-U6-human (target1) ZEB1 sgRNA-SFFV-Cas9 nuclease-2A-Puro (#K2671006, Applied Biological Materials) or pLenti-U6-Scrambled sgRNA-SFFV-Cas9 nuclease-2A-Puro (#K010, Applied Biological Materials)]. The pCMVdeltaR8.91 and phCMVG-VSVG vectors are gifts of Didier Nègre (International Center for Infectiology Research, Inserm U1111 - CNRS UMR5308 - ENS de Lyon - UCB Lyon1, EVIR Team, Lyon, France). 48 hours post-transfection, the supernatant was collected, filtered, supplemented with 5 µg/ml of polybrene (Sigma) and combined with the targeted cells for 6 hours. 48 hours following the infection cells were selected with puromycin (1 mg/ml). After transduction and antibiotic selection cells were cultured in limit dilution conditions to obtain single cells and then clonal populations.

ZEB1 CRISPR Genomic Cleavage Detection. Confirmation of successful ZEB1 gene editing was obtained with the CRISPR Genomic Cleavage Detection Kit (#G932, Applied Biological Materials). CRISPR edited samples were used as a template in PCR reactions targeting the ZEB1 specific region of interest. The products were then denatured and reannealed to produce mismatches within the double strand. A detection enzyme was able to recognize such mismatches and cleaves the strands to produce band sizes that are distinguishable upon gel analysis.

Immunohistochemistry analysis

For immunohistochemical analyses (IHC), we used a cohort of 154 formalin-fixed paraffin-embedded (FFPE) lung cancer specimens that included 52 ADC and 47 SqCC and 55 SC that were collected from patients who underwent surgical resection in the Department of Thoracic Surgery at Grenoble University Hospital or at the Nice University Hospital. All cases were well characterized in terms of clinical and pathological features. The Ethics Committees from each institution approved this study.

IHC staining was performed using an automated immunostainer (Benchmark Ultra, Roche, Meylan, France) on full tumor sections from FFPE blocks using antibodies against CD70 Abcam, ab133398), ZEB1 (BETHYL Laboratories, IHC-00419), CD3 (Roche Diagnostics, 5278422001), CD8 (Roche Diagnostics, 5937248001) and FOXP3 (Abcam, ab99963). Microscopic quantification of expression was used to calculate the H- score (% of positive cells x intensity ranging from 1 to 3). Expression scores were based on the whole section examination, by an expert thoracic pathologist (SL). The number of cells per mm^2 expressing CD3, CD8 and FOXP3 were also quantified using the Cytonuclear IHC module of the HALO Image analysis Platform (Indica Labs, USA).

Bioinformatics and Statistical analyses

Bioinformatics analyses were performed using the Array Studio software (Omicsoft Corporation, Research Triangle Park, NC, USA) and the R language. Raw data from affymetrix microarrays were processed using quantile normalization and the robust multi-array average (RMA) algorithm and were log2 transformed [21]. For samples from TCGA, we downloaded normalized read counts (RPKM) that we then log2 transformed.

Unsupervised hierarchical cluster analysis of CCLE cell lines with ICPLs was performed using the Pearson correlation coefficient and Ward linkage method. In each dataset included in the study, gene expression levels of CD70 and EMT-TFs: ZEB1/ZEB2, SNAI1/SLUG, TWIST1/TWIST2 were extracted. Using the single-sample Gene Set Enrichment Analysis (ssGSEA) tool [21–23], we computed in each sample an enrichment score (ES) of a previously published pancancer EMT signature [11], including 52 and 25 genes overexpressed and underexpressed respectively in mesenchymal compared to epithelial samples. Using this tool, the gene expression values for a given sample were rank-normalized, and an ES was produced using the empirical cumulative distribution functions of the genes in the gene signature and the remaining genes. The EMT score was computed as the following: ES_{UP} genes – ES_{DN} genes. Thus, consistently with previous description of the signature, samples with a negative score were classified “epithelial” whereas a positive score defined “mesenchymal” samples. Summary

statistics, including median and range values, were used to describe the distribution of genes in different datasets. In the CCLE dataset, groups were compared using the Kruskal-Wallis test. In both cases, a q-value was computed to take into account multiple comparisons.

Statistical analyses were conducted using GraphPad Prism version 7.0 (GraphPad). An unpaired t test was used for comparisons between two-group means, where the data could be assumed to have been sampled from populations with normal (or approximately normal) distributions. All P values were two tailed, and for all analyses, $P < 0.05$ was considered statistically significant. To assess significant correlations between *CD70*, the EMT-related transcription factors of the EMT-pancancer signature, a Spearman's correlation was performed.

RESULTS

CD70 expression is elevated in mesenchymal non-small cell lung cancer cell lines

Gene expression levels of 12 immune-checkpoint ligands (ICPLs) were evaluated across 130 NSCLC cell lines from the cancer cell line encyclopedia (CCLE) and subjected to unsupervised clustering analysis (**Fig. 1a**). Three prominent broad clusters were observed on the basis of significantly high ICPL expression and included *CD70* (TNFSF7), *CD274* (PD-L1) and *VTCN1* (B7H4). Since increased expression of immune checkpoints and other druggable immune targets has been correlated with EMT in a variety of human cancers [11]; we determined whether the pattern of ICPLs expression we observed was associated with the acquisition of mesenchymal properties in NSCLC cell lines.

Assessment of the epithelial or mesenchymal status of these cell lines was performed with the single sample Gene Set Enrichment Analysis (ssGSEA) tool, using a patient-derived EMT signature reported previously [11]. Using this signature, mesenchymal cells are defined by an EMT score > 0. We observed that mesenchymal cells (n=32) expressed significantly higher levels of *CD70* when compared to epithelial NSCLC cell lines (n=98; Mann Whitney Test $P < 0.0001$, **Fig. 1b**). *TNFSF4* (OX40L) was also increased in mesenchymal NSCLC cell lines

(**Supplementary Figure 1A**, Mann Whitney Test $P < 0.0001$). *CD274* was not differentially expressed between epithelial and mesenchymal NSCLC cell lines, and expression of *VTCN1* was enriched in epithelial cells (**Supplementary Figure 1A**). Increased *CD70* expression was also confirmed in a set of 112 non-overlapping cell lines (55 epithelial and 57 mesenchymal) from the GSE32036 dataset (**Supplementary Figure 1B**).

To confirm that mesenchymal cell lines harbor increased levels of CD70, the EMT status of 4 selected NSCLC cell lines was evaluated through the analysis of the protein levels of known epithelial and mesenchymal markers. Consistently with microarray data (**Fig. 1a**), H3255 and H441 cells presented an epithelial phenotype while HCC44 and H23 were mesenchymal (**Fig. 1c**). To assess whether CD70 was associated with the mesenchymal status in these cell lines, we analyzed CD70 protein expression by flow cytometry. In line with the *in silico* data, our results evidenced higher CD70 expression in the mesenchymal HCC44 and H23 cell lines (MFI of 23.8 and 28.9, respectively) compared to cell lines with epithelial phenotype (MFI of 3.8 and 3.9, respectively, **Fig. 1d,e**). Further, gene reporter assays demonstrated that the activity of the human *CD70* promoter was increased in the HCC44 cell line (mesenchymal) when compared to the H3255 (epithelial) (**Supplementary Figure 1C**).

Analysis of publicly available data in the GEO database on the time-dependent global gene expression during TGFβ-induced EMT (GSE17708) yielded concurrent findings of increased *CD70* expression in the A549 NSCLC cell line (intermediate mesenchymal) after 72 hours of treatment with TGF-β (**Supplementary Figure 1D**). Finally, a slight increase in CD70 expression was observed in a model of acquired resistance to erlotinib, derived from the HCC4006 NSCLC cells, that undergo EMT in a TGF-β-independent fashion [24,25] (**Supplementary Figure 1E,F**).

Collectively, these results suggest that CD70 is highly expressed in mesenchymal NSCLC cell line models.

Modulation of ZEB1 expression *in vitro* impacts CD70 expression

The transcription factor ZEB1 is a master inducer of EMT and invasiveness, tumor initiation and cancer cell plasticity [14]. ZEB1 drives drug adaptation and phenotypic resistance to MAPK inhibitors in melanoma [9] and EMT-related acquired resistance to EGFR inhibitors in lung adenocarcinomas [25]. Moreover, ZEB1 expression has been shown to be an early, critical event in lung cancer pathogenesis [26]. Based on these observations we hypothesized that ZEB1 modulation *in vitro* played a role in CD70 expression.

We used publicly available transcriptome sequencing data from an *in vitro* model of pre-neoplastic human bronchial epithelial cells (HBECs) that were genetically manipulated to overexpress ZEB1 ($HBEC^{ZEB1}$) [26]. We evaluated the EMT score [11] for the $HBEC^{ZEB1}$ cells as well as for their corresponding isogenic cells ($HBEC^{pMSCV}$), as indicated previously [11]. We confirmed that $HBEC^{pMSCV}$ cells were "epithelial" and that expression of ZEB1 in the $HBEC^{ZEB1}$ cells resulted in a shift towards a "mesenchymal" score (**Fig. 2a**). Interestingly, we found that *CD70* was the 9th most differentially expressed gene in $HBEC^{ZEB1}$ when compared with the $HBEC^{pMSCV}$ (**Fig. 2b**), after genes involved in histone hyperacetylation, metabolism of corticosteroids, cell differentiation, cell adhesion, migration, angiogenesis, tissue morphogenesis and growth suppression.

In order to study the effect of ZEB1 modulation on the expression of CD70 *in vitro*, we generated a CRISPR/Cas9-mediated knockdown of ZEB1 in HCC44 cells (lung cancer, mesenchymal) (**Supplementary Figure 2**). *ZEB1* knockdown resulted in a strong decrease in ZEB1 expression and up-regulation of E-cadherin, a known epithelial marker, in the three HCC44 sgZEB1 clones, when compared to the control (**Fig. 2c**). In line with our *in silico* observations, CD70 expression was down regulated in the sgZEB1 clones #1 and #2 (MFI of 15.2 and 28.2, respectively) compared to the control MFI of 42.7, **Fig. 2d**). In sgZEB1 clone #3 the change in CD70 expression, when compared to control, was not significant (**Fig. 2d**). As an orthogonal experiment, we used a lentiviral system to overexpress ZEB1 in the epithelial PC9 lung cancer cell line. In this model, ZEB1 overexpression was observed at the mRNA and protein levels were observed, when compared to control, and was coupled with an increase of the mesenchymal marker, vimentin (**Fig. 2e**). Further, increased ZEB1 expression resulted in the

activation of the human *CD70* promoter (**Fig. 2f**) and a subsequent increase in *CD70* mRNA expression (**Fig. 2g**), when compared to control PC9 cells.

Overall, these observations demonstrate that ZEB1 regulates the expression of *CD70* in NSCLC *in vitro*.

Inhibition of CD70 expression *in vitro*

To investigate the impact of modulating CD70 expression in mNSCLC *in vitro*, we assessed the expression of EMT-related factors, as well as the transcriptional changes and their predicted networks after silencing CD70 (siRNA) in $CD70^{HIGH}$ mesenchymal lung cancer cell lines. CD70 knock-down resulted in increased expression of Zeb1 in HCC44 cells, which was not observed in H23 cells (**Fig. 3a**). The expression of vimentin was not altered upon CD70 silencing.

Differential gene expression analyses in HCC44 cells evidenced 118 upregulated and 158 downregulated genes upon *CD70* knockdown in HCC44 cells (Log2FC > 0, adjusted p-value > 0.05). CD70 deregulation, in both HCC44 and H23 cells, was associated with decreased expression of Gasdermin B (*GSDMB*), which is implicated in the regulation of apoptosis in epithelial cells and constitutes a key downstream mediator of granzyme-mediated cell death. Following *CD70* knockdown, HCC44 cells displayed increased expression of *TNFSF10* (TNF ligand superfamily member 10), involved in cancer cell apoptosis by binding to and activating signaling by trimeric death receptors; and *VCAM1* (Vascular Cell Adhesion Molecule 1) which mediates leukocyte-endothelial cell adhesion and signal transduction.

Top modulated pathways showed that silencing CD70 in HCC44 cells results in enrichment of cellular programs associated with DNA repair, DNA replication, glycolysis, TNF-alpha signaling and angiogenesis (**Fig. 3b**), while transcriptomic signatures of regulation of double-strand break repair were diminished. Intriguingly, and in line with the ZEB1 protein expression pattern observed previously (**Fig. 3a**), *CD70* silencing was associated with an enrichment of an EMT signature in HCC44 cells, potentially suggesting a feedback loop and reciprocal regulation between CD70 and ZEB1 in this model.

While these data are limited, they suggest that CD70 might be implicated in molecular processes associated to granzyme-mediated cell death, DNA repair, angiogenesis and glycolysis, in mesenchymal lung cancer models.

Increased CD70 expression is observed in mesenchymal lung carcinomas

To study the expression of *CD70* in "epithelial" and "mesenchymal" NSCLC, mRNA expression data from the lung adenocarcinoma (ADC) and lung squamous cell carcinoma (SqCC) TCGA datasets were analyzed. The EMT status was assessed according to the EMT pan-cancer signature reported previously [11]. Consistent with our findings in cell lines, we evidenced significantly higher levels of *CD70* mRNA expression in mesenchymal tumors as compared with epithelial tumors in both lung ADC (Mann Whitney Test $P<0.0001$, **Fig. 4a**) and lung SqCC (Mann Whitney Test $P<0.0001$, **Fig. 4b**). In line with these results, we evidenced a significant correlation between *CD70* and the expression levels of the EMT transcription factors *ZEB1/2, TWIST1/2* and *SNAI1* (**Supplementary Table S1**). Moreover, the expression of *CDH1*, an epithelial marker, negatively correlated with *CD70* mRNA expression in these datasets (**Supplementary Table S1**).

The significant increase in *CD70* expression observed in mesenchymal lung ADC was validated in an independent dataset (GSE41271) (Mann Whitney Test $P<0.0001$, **Fig. 4c**), where we also observed a non-significant trend towards higher *CD70* expression in mesenchymal SqCC when compared with epithelial SqCC (Mann Whitney Test $P=0.064$, **Fig. 4c**). Interestingly, in this dataset, *CD70* expression was particularly higher in the group of pulmonary sarcomatoid carcinomas (n=4) when compared to other mesenchymal NSCLC ($P<0.01$, **Fig. 4c**). Further, *CD70* expression proved to be enriched in lung tumors when compared to normal pulmonary tissue in three independent datasets (**Fig. 4d**).

Taken together, our data suggests that mesenchymal lung tumors, and in particular pulmonary sarcomatoid carcinomas, show increased levels of *CD70* mRNA expression compared epithelial lung tumors.

Increased CD70 expression in pulmonary sarcomatoid carcinomas is associated with the presence of cancer cells with a mesenchymal phenotype

Sarcomatoid carcinomas of the lung are rare tumors with an incidence estimated between 2% to 3% of all lung malignancies [27–29]. These tumors are characterized by the presence of spindle cell elements (spindle cell sarcomatoid carcinomas) or giant cells (giant cell sarcomatoid carcinomas) or a mix of spindle and giant cells. Among sarcomatoid carcinomas, pleomorphic carcinomas are characterized by a mix of "differentiated" components such as adenocarcinoma, squamous cell or large cell carcinoma, with either spindle cell or giant cell carcinomas [29,30].

We studied a series of in 154 formalin-fixed paraffin-embedded (FFPE) lung cancer specimens that included 52 ADC, 47 SqCC and a large cohort of 55 pulmonary sarcomatoid carcinomas (SC), all for which we had full tumor sections of high quality for immunohistochemical analysis. All tumors were thoroughly analyzed, and the histological features of pulmonary SC were confirmed by an expert pathologist, according to the 2015 WHO classification.

Immunohistochemical staining and scoring of ZEB1 expression in tumor cells showed significantly increased expression levels of ZEB1 in SC tumors as compared to ADC or SqCC (**Fig. 5a**). In the latter, nuclear ZEB1 staining was mainly restricted to stromal fibroblasts and endothelial cells (**Fig. 5a**). Using targeted RNA sequencing of 2,559 genes, we calculated the transcriptional EMT signature in a subset of these samples (51 ADC, 44 SqCC and 40 SC), for which sequencing analyses were possible. Although the overlap between the gene lists of the EMT pancancer signature [11] and the panel used for targeted RNA sequencing was 38.5%, the EMT signatures calculated with these gene lists were highly and significantly correlated in the CCLE NSCLC (r=0.986, P <0.0001), ADC TCGA (r=0.981, P <0.0001) and SqCC TCGA datasets (r=0,892, P <0.0001) (**Supplementary Figure 3A**). Using this signature, we observed that, in line with the immunohistochemistry results obtained for ZEB1 (**Fig. 5a**), pulmonary spindle-cell SC presented higher EMT signature scores than lung ADC or lung SqCC (P < 0.0001, **Fig. 5b**), thus confirming the mesenchymal nature of these tumors.

Our *in silico* analyses previously evidenced increased levels of *CD70* mRNA expression in "mesenchymal"-like NSCLC (**Figs. 5a-c**). Consistent with these results, we found that *CD70*

mRNA expression presented the strongest positive and significant correlation with EMT (r = 0.560, $P < 0.0001$) among the ICP(L)s included in the targeted RNA-sequencing panel used, followed by *PDCD1LG2* (PD-L2), *CD276* (B7H3) and *HAVCR2* (TIM3) (**Supplementary Figure 3B**, **Supplementary Table S2**). Noteworthy *CD70* mRNA expression was also positively and significantly correlated with *ZEB1* expression and other EMT-transcription factors, as well as negatively correlated with *CDH1* expression (**Fig. 5c**, **Supplementary Table S3**).

Concordantly, immunohistochemical analyses revealed a significantly higher proportion of cases expressing CD70 among SC (68%), as compared to lung ADC (56%) or lung SqCC (47%) (P=0.010, **Fig. 5d**). Of note CD70 staining was localized in the membrane and was restricted to tumor cells (**Fig. 5d**).

Then, we analyzed a small cohort of pleomorphic SC (P, n=11). Detailed pathology review of these samples allowed us to perform targeted RNA sequencing in the spindle cell (SP) and epithelial (E) components separately. We observed that the SP component was significantly more “mesenchymal”-like than the paired epithelial component (P = 0.009, **Fig. 5e**), which was consistent with the immunohistochemistry analyses that showed that, in 10 out of 11 samples, ZEB1 expression was significantly enriched in the SP component when compared to the paired epithelial (E) component (**Fig. 5f**). Interestingly, a similar pattern was observed for the expression of CD70, in 9 out of 11 samples (**Fig. 5g**).

Although co-localization of the ZEB1 and CD70 signals was not performed, as double staining methodology was not used, our results suggest that CD70 is frequently expressed in pulmonary SC and is particularly enriched in the mesenchymal elements present in carcinomas that belong to the pleomorphic subclass.

CD70 expression is associated with traits of an immunosuppressive microenvironment in pulmonary sarcomatoid carcinomas

To determine whether the increased CD70 expression observed in pulmonary SC was coupled with an immunosuppressive tumor microenvironment, full tumor sections were stained and automatically quantified for CD3 and CD8 expression. This analysis revealed that pulmonary

SC expressing high CD70 levels displayed significantly decreased infiltration by $CD3^+$T-cells (**Fig. 6a,c**) and $CD8^+$Tcells (**Fig. 6b,c**). No significant differences in CD3 and CD8 expression were observed in ADC and SqCC, according to their CD70 status (**Supplementary Fig. 5a,b**). The constitutive expression of CD70 by tumor cells may facilitate evasion of the immune system by three mechanisms: i) skewing T cells towards T cell exhaustion, ii) increasing the amount of suppressive regulatory T cells (Tregs) or iii) inducing T cell apoptosis [31–33]. Using the targeted transcriptome data derived from the overall cohort of ADC, SqCC and SC cases, we evaluated the expression of genes coding for the inhibitory receptors PD1 (*PDCD1*), LAG3 and TIM3 (*HAVCR2*), known to be involved in T-cell exhaustion [34] and evidenced a positive and significant correlation of *CD70* with the three markers (**Fig. 6d**, **Supplementary Table S4**). The expression of *FOXP3*, an established marker of Tregs, was positively and significantly correlated with *CD70* at the mRNA level in the overall cohort (**Fig. 6e**). However, these observations were not validated by immunohistochemistry analyses of FOXP3 protein expression (**Supplementary Figures 4,5c**). We observed, though, a non-significant trend towards increased FOXP3 protein in $CD70^{HIGH}$ ADC (**Supplementary Figure 5d**).

To gain further insights into the tumor microenvironment of CD70-positive tumors, we assessed immune population infiltration scores, as defined by MCP-counter [35]. This approach revealed a positive and significant association between CD70 expression and infiltration by NK cells in pulmonary SC (**Fig. 6f**); while in ADC and SqCC, NK cells infiltrate was less abundant in $CD70^{HIGH}$ tumors (**Supplementary Fig. 5e**). This immune infiltrate deconvolution analysis also showed that $CD70^{HIGH}$ pulmonary sarcomatoids present a week proportion of neutrophils (**Fig. 6f**). Assessment of a potential NK cell-associated exhausted phenotype in $CD70^{HIGH}$ tumors was hindered by the fact that the genes coding for NKG2D, CD16/Fc gamma RIII, CD94-NKG2C, NKp30, NKp44, NKp46, or NKp80, specific activating receptors of NK cells, were not present in the targeted-transcriptome panel.

Taken together, our data provide evidence that $CD70^{HIGH}$ pulmonary SC display features of an immunosuppressive microenvironment as evidenced by decreased CD3+ and CD8+ T-cell

infiltration. CD70^{HIGH} lung tumors are also characterized by enhanced mRNA expression of markers of T cell exhaustion.

DISCUSSION

Herein, we provide evidence that EMT promotes immune escape by inducing CD70 expression in lung cancer mesenchymal cell lines and patient samples. Notably, we found that the modulation of *ZEB1* impacts CD70 expression and results in an increased activity of the human *CD70* promoter *in vitro*. Moreover, our results reveal that CD70 expression is particularly enriched in pulmonary sarcomatoid carcinomas, a rare subtype of highly aggressive and poorly differentiated NSCLC, chemoresistant to platinum-based standard regimens and with a particularly poor prognosis [28,36,37].

CD70 is a type-II transmembrane glycoprotein that belongs to the tumor necrosis factor (TNF) superfamily [31]. In adoptive cell transfer models, mechanistic analyses revealed that IFN-γ induces CD70 expression on T cells, and that CD70 limits T cell expansion via caspase-dependent T cell apoptosis and upregulation of inhibitory immune checkpoint molecules [38]. More recently, it was demonstrated that CD70 regulates migration and invasion of mesothelial and mesothelioma cells and that CD70 worsens the prognosis of mesothelioma transplanted mice via enhanced invasiveness and immune evasion [39]. Finally, in solid tumors, the CD70/CD27 pathway has been shown to induce T cell apoptosis and exhaustion and is associated with increased tumor aggressiveness [31,33].

To better understand the cellular pathways and programs involving CD70, we modulated the expression of CD70 (siRNA) in mesenchymal lung cancer cell lines. CD70 knockdown was associated with the enrichment of transcriptomic signatures related to angiogenesis and WNT β-catenin signaling. Conversely, CD70 is reported to have a regulatory role in hypoxia in glioblastoma [40,41] and to induce Wnt pathway activation upon ligation of CD27 in leukemia stem cells [42], thus likely indicating that CD70 involvement in these cellular processes might be cell-

type dependent. Unlike H23 cells, CD70 inhibition resulted in increased ZEB1 expression and enrichment of the epithelial-to-mesenchymal signature in HCC44 cells. A recent study showed that CD70 silencing depressed pathways related to EMT signaling in glioblastoma cell lines [40]. These results potentially suggest that, in some *in vitro* models, CD70 might impact the expression of ZEB1 *via* a regulatory feedback loop. The relevance of these observations *in vivo* or in patients remains to be determined.

Common mechanisms regulate EMT induction and tumor immune escape [10,13,43,44]. Indeed ZEB1, a key driver of EMT in lung cancer [15], is known to relieve *miR-200* repression of PD-L1 on lung tumor cells, leading to $CD8^+$ T-cell immunosuppression and lung cancer metastasis [13]. In line with these observations, an increase in tumor-infiltrating $CD4^+FOXP3^+$ Tregs was reported in patients with "mesenchymal" lung adenocarcinoma in contrast to those with an "epithelial" phenotype [10]. Chen *et al*. previously demonstrated the molecular link between EMT and intratumoral $CD8^+$ T cell suppression *in vivo* and *in vitro*[13]. In another study, a high EMT transcriptional score was associated with lower CD4 T cell infiltration in lung ADC, lower intratumor $CD4^+/CD8^+$ T cell ratio in lung SqCC, as well as higher infiltration by activated B cells and Tregs in both lung ADC and SqCC [44]. Furthermore increased TGFβ, a known EMT inducer, in the tumor microenvironment was reported to be a primary mechanism of immune evasion by promoting T-cell exclusion, in metastatic colorectal cancer [45].

In our study, immunohistochemical analysis of a large cohort of pulmonary SC revealed that increased CD70 expression is coupled with a decreased $CD3^+$ and $CD8^+$ T cell infiltrate. Interestingly, targeted-transcriptome analyses evidenced that *CD70* expression is associated with increased expression of T cell exhaustion markers, at mRNA level. Therefore, the association of EMT and CD70 in lung tumors may denote an important role of this interaction in immune escape. In these tumors, EMT might therefore promote cancer growth and metastasis not only by increasing the plasticity of cancer cells, but also by reprogramming the immune response in the local tumor microenvironment.

CD70 expression in tumor cells has been suggested to enhance immune evasion and accelerate tumor growth through several distinct mechanisms, including expansion of $FOXP3^+$

regulatory T-cells (Tregs) [46], as demonstrated in non-Hodgkin lymphoma [47], glioblastoma [33] and, more recently, in malignant pleural mesothelioma [39]. In contrast with these reports, we did not observe increased FOXP3 protein expression in CD70^{HIGH} lung tumors, despite having found a positive correlation between *CD70* and *FOXP3* in these samples, at the mRNA level.

Neutrophils are the most abundant immune cell population in the NSCLC tumor microenvironment [48]. Neutrophils have the capacity to sustain EMT, inhibiting metastasis initiation [49]. Contrastingly, a recent study revealed that neutrophils induce expression of zinc-finger protein SNAI1 and promote EMT in cancer cells, fostering the invasion and further recruitment of neutrophils in a mouse model of lung cancer [50]. Neutrophils can also foster anticancer responses, as illustrated by the identification of neutrophils with an antigen-presenting cell-like phenotype, which trigger antitumor T cell responses in human lung cancer [49,51]. Deconvolution analysis indicated that CD70^{HIGH} pulmonary SC present a low intratumoural neutrophil content. Supplementary validation using flow cytometry and immunohistochemistry staining for CD66b will allow to comprehensively profile the neutrophil content and function present in these tumors.

Increased CD70 expression was associated with enhanced NK cell infiltrate in pulmonary SC, as evaluated using RNA sequencing data. Al Sayed *et al.,* demonstrated a critical role for CD70 signaling in the capacity of NK cells to eliminate lymphoma cells [52]. More recently, Riether *et al.,* provided evidence that cusatuzumab, a first-in-class, high-affinity anti-CD70 monoclonal antibody, further reduced leukemia engraftment and leukemia stem cells numbers in the bone marrow and spleen in the presence of NK cells (derived from the buffy coats of healthy donors), compared to anti-CD70 alone [53]. Further investigation is warranted to validate the enriched NK cells infiltration in CD70^{HIGH} lung tumors, and to assess their contribution to the immune phenotype of these tumors.

CD70 expression on tumor cells has been suggested to contribute to tumor cell immune evasion of tumor cells through T-cell apoptosis [33,54,55], Treg expansion [32,56] and T-cell exhaustion [57]. In the context of our observations and based on prior reports [58–60], we hypothesize that

persistent delivery of costimulatory signals via CD27-CD70 interactions in memory T-memory cells can participate to their exhaustion.

Cusatuzumab has shown potent cytotoxic effects on $CD70^{+}$ NSCLC cell lines [61]. The dose-escalation phase I trial provided evidence of good tolerability of cusatuzumab and antitumor activity in heavily-treated patients with advanced CD70-positive tumors [62]. Recent data from the phase 1 dose escalation part of the ongoing phase 1/2 clinical trial (NCT03030612) evaluating cusatuzumab in combination with azacytidine in acute myeloid leukemia (AML) reported that combination treatment is highly active in previously untreated patients with AML and unfit for intensive chemotherapy (median time to response: 3.3 months; median PFS not reached) [63]. Interestingly, in this setting, cusatuzumab eliminated CD70-expressing leukemia stem cells resulting in deep and durable remissions [63].

We performed preliminary analyses using an *ex vivo* culture system, in which serial sections of patient-derived lung cancer fresh tumors were cultured either in the presence or in the absence of cusatuzumab (**Supplementary Data and Supplementary Fig. 6**). In a $CD70^{HIGH}$ lung adenocarcinoma sample, anti-CD70 treatment had a cytotoxic effect and resulted in the retention of CD3+ tumor-infiltrating lymphocytes and an increase in the concentration of soluble IFN-γ and Granzyme A, compared to control, indicative of a partial reversion of the immunosuppressive phenotype initially present in the treatment-naïve sample (**Supplementary Data and Supplementary Figs. a – d**). We observed that the magnitude of these effects was minor, upon cusatuzumab treatment, in a second lung adenocarcinoma sample that displayed a lower intensity of CD70 positivity (**Supplementary Data and Supplementary Fig. e - h**). Further confirmation of these observations is needed in a larger number of samples and, notably, in $ZEB1^{HIGH}/CD70^{HIGH}$ NSCLC or in pulmonary sarcomatoid carcinomas.

Research focusing on the molecular events that that underline the development of pulmonary sarcomatoid tumors is scarce and thus has prevented the development of specific treatment strategies [20,64]. Since pulmonary SC are characterized by a higher rate of resistance to conventional chemotherapy than other NSCLCs [36,65,66], these tumors currently represent a relevant clinical challenge.

Loss of the epithelial-associated transcription factor OVOL2 characterizes the transition to sarcomatoid phenotype *via* the EMT-TFs TWIST and ZEB, and the expression of the membrane kinase DDR2. In this context, dasatinib was reported to restrain cell proliferation *in vitro* and to revert the sarcomatoid-associated phenotype [67]. A report on the efficacy of anti-PD(L)-1 immunotherapy in pulmonary SC showed that patients present an ORR of 40.5% and an OS of 12.7 months, suggesting that patients with pulmonary SC are likely to be very good candidates for immune checkpoint inhibitor therapy [68].

Genetic characterization of pulmonary SC revealed that high mutational burden and that mutations in *KRAS* are associated with poor prognosis and decreased patient survival [69]. Moreover, *MET* exon 14 alterations are enriched in pulmonary SC compared to other NSCLC tumors. We evidenced that combined MET and PIK3CA pharmacological inhibition induces early activation of CD70, coupled with increased ZEB1 expression in a lung cancer mesenchymal cell line (**Supplementary Data and Supplementary Fig. 7a**). In chronic myelogenous leukemia BCR-ABL1-targeted therapy was reported to induce the expression of CD70 in leukemia stem cells by down-regulating microRNA-29, resulting in reduced CD70 promoter DNA methylation. As a consequence, CD70 triggered CD27 signaling and compensatory Wnt pathway activation [53]. The relevance of our observations in patient-derived models and the biological consequences of CD70 activation in early response to targeted therapy in mesenchymal lung tumors, warrants further investigation.

This study provides evidence of CD70 overexpression in a subgroup of patients with pulmonary SC, together with preliminary proof of CD70 activation in early response to combined MET/PIK3CA targeted therapy in lung cancer mesenchymal model. These results suggest that CD70 might be a potential pathway to explore for therapeutically targeting lung mesenchymal tumors, in particular pulmonary SC, with immunotherapy. Cusatuzumab, which blocks CD70/CD27 signaling by binding to human CD70, has shown promising activity in advanced solid tumors [62,70], glioblastoma [40], acute myeloid leukemia [63] and refractory cutaneous T- cell lymphoma [71]. In addition, a phase 1, dose-escalation study (NCT00944905) to define the safety profile of MDX-1203, an anti-CD70 drug conjugate, was recently completed in subjects with

CD70-positive advanced or recurrent clear cell renal cell carcinoma or B-Cell Non-Hodgkin's Lymphoma. CD70 expression on cancer cells is an attractive candidate for targeted immunotherapy due to its limited expression on non-malignant cells; an observation that was confirmed in our study. Therefore, targeting CD70 in CD70-expressing tumors might potentially offer treatment perspectives for mesenchymal lung cancers.

DATA AVAILABILITY

The data that support the findings of this study are available from the authors upon request.

FUNDING

This work was mainly supported by the French National Cancer Institute (INCa) Biology and Basic Sciences for Cancer research grant PLBIO15-266 (P.S., S.O.C., A.P., C.C., S.L.) (2015-2019) and the LYriCAN Grant INCa-DGOS-Inserm_12563. S.O.C. was supported by a post-doctoral fellow grant from Fondation de France (2015-00060226). MR is supported by the Ecole de l'Inserm Liliane Bettencourt. P.S. is supported in part by Institute Roche. A.S. was supported by a 2014-2015 clinical fellowship award for a Master degree from Saint-Etienne Jean Monnet University.

ACKNOWLEDGEMENTS:

This work has been developed and supported through the FHU OncoAge consortium. The authors thank C. Lovly (U. Vanderbildt, USA) and R. Thomas (U. Cologne, Germany) for kindly providing some of the cell lines used in this study; Suzanne André and Amélien Sanlaville for their help with FACS analyses; Xavier Huet and Céline Rodriguez for their help with cytokine dosage, and Jenny Valadeau-Guilemond for the fruitful discussions.

AUTHORS CONTRIBUTIONS

Conception and design: SO-C, AS, AP, PS

Development of methodology: SO-C, AS, APM, AP, PS

Acquisition of data (provided animals, acquired and managed patients, provided facilities, etc.): SO-C, AS, JPF, AD, SM, MB, CL, NM, APM, FF, MR, RP, MAA, GDS, NG, VA, CA, LM, SL, AT, LT, LM, MG, SL, AT, LT, SB, CMC, SB, QW, MP, CC, PH, SL, AP, PS.

Analysis and interpretation of data (e.g., statistical analysis, biostatistics, computational analysis): SO-C, AS, JPF, MB, APM, FF, MR, LM, SL, AT, LM, MG, SL, AT, LT, SB, LT, SB, RMP, CMC, CC, PH, SL, AP, PS.

Writing, review, and/or revision of the manuscript: SO-C, AS, APM, CMC, PH, SL, AP, PS

Administrative, technical, or material support (i.e., reporting or organizing data, constructing databases): FB, VA, PH, SL,

Study supervision: SO-C, AP, PS

REFERENCES

1 Brahmer J, Reckamp KL, Baas P, Crinò L, Eberhardt WEE, Poddubskaya E *et al.* Nivolumab versus Docetaxel in Advanced Squamous-Cell Non–Small-Cell Lung Cancer. *N Engl J Med* 2015; **0**: null.

2 Gettinger S, Rizvi NA, Chow LQ, Borghaei H, Brahmer J, Ready N *et al.* Nivolumab Monotherapy for First-Line Treatment of Advanced Non-Small-Cell Lung Cancer. *J Clin Oncol* 2016. doi:10.1200/JCO.2016.66.9929.

3 Herbst RS, Baas P, Kim D-W, Felip E, Pérez-Gracia JL, Han J-Y *et al.* Pembrolizumab versus docetaxel for previously treated, PD-L1-positive, advanced non-small-cell lung cancer (KEYNOTE-010): a randomised controlled trial. *Lancet* 2016; **387**: 1540–1550.

4 Borghaei H, Paz-Ares L, Horn L, Spigel DR, Steins M, Ready NE *et al.* Nivolumab versus Docetaxel in Advanced Nonsquamous Non-Small-Cell Lung Cancer. *N Engl J Med* 2015; **373**: 1627–39.

5 Ribas A, Wolchok JD. Cancer immunotherapy using checkpoint blockade. *Science* 2018; **359**: 1350–1355.

6 Zhang T, Guo L, Creighton CJ, Lu Q, Gibbons DL, Yi ES *et al.* A genetic cell context-dependent role for ZEB1 in lung cancer. *Nat Commun* 2016; **7**: 12231.

7 Thomson S, Buck E, Petti F, Griffin G, Brown E, Ramnarine N *et al.* Epithelial to mesenchymal transition is a determinant of sensitivity of non-small-cell lung carcinoma cell lines and xenografts to epidermal growth factor receptor inhibition. *Cancer Res* 2005; **65**: 9455–9462.

8 Morel A-P, Hinkal GW, Thomas C, Fauvet F, Courtois-Cox S, Wierinckx A *et al.* EMT Inducers Catalyze Malignant Transformation of Mammary Epithelial Cells and Drive Tumorigenesis towards Claudin-Low Tumors in Transgenic Mice. *PLoS Genet* 2012; **8**: e1002723.

9 Richard G, Dalle S, Monet M, Ligier M, Boespflug A, Pommier RM *et al.* ZEB1-mediated melanoma cell plasticity enhances resistance to MAPK inhibitors. *EMBO Mol Med* 2016; **8**: 1143–1161.

10 Lou Y, Diao L, Cuentas ERP, Denning WL, Chen L, Fan YH *et al.* Epithelial-Mesenchymal Transition Is Associated with a Distinct Tumor Microenvironment Including Elevation of Inflammatory Signals and Multiple Immune Checkpoints in Lung Adenocarcinoma. *Clin Cancer Res* 2016; **22**: 529–553.

11 Mak M, Tong P, Diao L, Cardnell RJ, Gibbons DL, William WN *et al.* A patient-derived, pan-cancer EMT signature identifies global molecular alterations and immune target enrichment following epithelial to mesenchymal transition. *Clin Cancer Res* 2015. doi:10.1158/1078-0432.CCR-15-0876.

12 Tripathi SC, Peters HL, Taguchi A, Katayama H, Wang H, Momin A *et al.*

Immunoproteasome deficiency is a feature of non-small cell lung cancer with a mesenchymal phenotype and is associated with a poor outcome. *Proc Natl Acad Sci U S A* 2016. doi:10.1073/pnas.1521812113.

13 Chen L, Gibbons DL, Goswami S, Cortez MA, Ahn Y-H, Byers LA *et al.* Metastasis is regulated via microRNA-200/ZEB1 axis control of tumour cell PD-L1 expression and intratumoral immunosuppression. *Nat Commun* 2014; **5**: 5241.

14 Puisieux A, Brabletz T, Caramel J. Oncogenic roles of EMT-inducing transcription factors. *Nat Cell Biol* 2014; **16**: 488–94.

15 Larsen JE, Nathan V, Osborne JK, Farrow RK, Deb D, Sullivan JP *et al.* ZEB1 drives epithelial-to-mesenchymal transition in lung cancer. *J Clin Invest* 2016; **126**: 3219–3235.

16 Nolte MA, Van Olffen RW, Van Gisbergen KPJM, Van Lier RAW. Timing and tuning of CD27-CD70 interactions: The impact of signal strength in setting the balance between adaptive responses and immunopathology. Immunol. Rev. 2009; **229**: 216–231.

17 Tesselaar K, Xiao Y, Arens R, van Schijndel GMW, Schuurhuis DH, Mebius RE *et al.* Expression of the Murine CD27 Ligand CD70 In Vitro and In Vivo. *J Immunol* 2003; **170**: 33–40.

18 Grewal IS. CD70 as a therapeutic target in human malignancies. *http://dx.doi.org.gate2.inist.fr/101517/14728222123341*http://www.tandfonline.com.gate2.inist.fr/doi/full/10.1517/14728222.12.3.341 (accessed 3 Jun2016).

19 Terra SBSP, Jang JS, Bi L, Kipp BR, Jen J, Yi ES *et al.* Molecular characterization of pulmonary sarcomatoid carcinoma: Analysis of 33 cases. *Mod Pathol* 2016; **29**: 824–831.

20 Schrock AB, Li SD, Frampton GM, Suh J, Braun E, Mehra R *et al.* Pulmonary Sarcomatoid Carcinomas Commonly Harbor Either Potentially Targetable Genomic Alterations or High Tumor Mutational Burden as Observed by Comprehensive Genomic Profiling. In: *Journal of Thoracic Oncology*. 2017, pp 932–942.

21 Balagopalan S, Ashok S, Mohandas KP. Viewing power flow in an electricity market as confluence of stable multilateral trades. *J Electr Syst* 2009; **5**: 1–21.

22 Barbie DA, Tamayo P, Boehm JS, Kim SY, Moody SE, Dunn IF *et al.* Systematic RNA interference reveals that oncogenic KRAS-driven cancers require TBK1. *Nature* 2009; **462**: 108–112.

23 Scott IAW, Workman PJ, Drayton GM, Burnip GM. First record of Bemisia tabaci biotype Q in New Zealand. *New Zeal Plant Prot* 2007; **60**: 264–270.

24 Suda K, Tomizawa K, Fujii M, Murakami H, Osada H, Maehara Y *et al.* Epithelial to mesenchymal transition in an epidermal growth factor receptor-mutant lung cancer cell line with acquired resistance to erlotinib. *J Thorac Oncol* 2011; **6**: 1152–61.

25 Yoshida T, Song L, Bai Y, Kinose F, Li J, Ohaegbulam KC *et al.* ZEB1 Mediates Acquired Resistance to the Epidermal Growth Factor Receptor-Tyrosine Kinase Inhibitors in Non-Small Cell Lung Cancer. *PLoS One* 2016; **11**: e0147344.

26 Larsen JE, Nathan V, Osborne JK, Farrow RK, Deb D, Sullivan JP *et al.* ZEB1 drives epithelial-to-mesenchymal transition in lung cancer. *J Clin Invest* 2016; **126**: 3219–35.

27 Rossi G, Cavazza A, Sturm N, Migaldi M, Facciolongo N, Longo L *et al.* Pulmonary carcinomas with pleomorphic, sarcomatoid, or sarcomatous elements: a clinicopathologic and immunohistochemical study of 75 cases. *Am J Surg Pathol* 2003; **27**: 311–324.

28 Mochizuki T, Ishii G, Nagai K, Yoshida J, Nishimura M, Mizuno T *et al.* Pleomorphic Carcinoma of the Lung. *Am J Surg Pathol* 2008; **32**: 1727–1735.

29 Weissferdt A, Kalhor N, Rodriguez Canales J, Fujimoto J, Wistuba II, Moran CA. Spindle cell and pleomorphic ("sarcomatoid") carcinomas of the lung: an immunohistochemical analysis of 86 cases. *Hum Pathol* 2017; **59**: 1–9.

30 Travis WD, Brambilla E, Burke AP, Marx A N. Pathology and Genetics of Tumours of the Lung, Pleura, Thymus and Heart. IARC Press, 2015, pp 88–94.

31 Jacobs J, Deschoolmeester V, Zwaenepoel K, Rolfo C, Silence K, Rottey S *et al.* CD70: an emerging target in cancer immunotherapy. *Pharmacol Ther* 2015. doi:10.1016/j.pharmthera.2015.07.007.

32 Claus C, Riether C, Schürch C, Matter MS, Hilmenyuk T, Ochsenbein AF. CD27 signaling increases the frequency of regulatory T cells and promotes tumor growth. *Cancer Res* 2012; **72**: 3664–76.

33 Wischhusen J, Jung G, Radovanovic I, Beier C, Steinbach JP, Rimner A *et al.* Identification of CD70-mediated apoptosis of immune effector cells as a novel immune escape pathway of human glioblastoma. *Cancer Res* 2002; **62**: 2592–9.

34 Pauken KE, Wherry EJ. SnapShot: T Cell Exhaustion. *Cell* 2015; **163**: 1038-1038.e1.

35 Becht E, Giraldo NA, Lacroix L, Buttard B, Elarouci N, Petitprez F *et al.* Estimating the population abundance of tissue-infiltrating immune and stromal cell populations using gene expression. *Genome Biol* 2016; **17**. doi:10.1186/S13059-016-1070-5.

36 Liu X, Jia Y, Stoopler MB, Shen Y, Cheng H, Chen J *et al.* Next-generation sequencing of pulmonary sarcomatoid carcinoma reveals high frequency of actionable MET gene mutations. *J Clin Oncol* 2016; **34**: 794–802.

37 Martin LW, Correa AM, Ordonez NG, Roth JA, Swisher SG, Vaporciyan AA *et al.* Sarcomatoid Carcinoma of the Lung: A Predictor of Poor Prognosis. *Ann Thorac Surg* 2007; **84**: 973–980.

38 O'Neill RE, Du W, Mohammadpour H, Alqassim E, Qiu J, Chen G *et al.* T Cell–Derived CD70 Delivers an Immune Checkpoint Function in Inflammatory T Cell Responses. *J*

Immunol 2017; **199**: 3700–3710.

39 Inaguma S, Lasota J, Czapiewski P, Langfort R, Rys J, Szpor J *et al.* CD70 expression correlates with a worse prognosis in malignant pleural mesothelioma patients via immune evasion and enhanced invasiveness. *J Pathol* 2020; **250**: 205–216.

40 Seyfrid M, Maich WT, Shaikh VM, Tatari N, Upreti D, Piyasena D *et al.* CD70 as an actionable immunotherapeutic target in recurrent glioblastoma and its microenvironment. *J Immunother Cancer* 2022; **10**: e003289.

41 Kitajima S, Lee KL, Fujioka M, Sun W, You J, Chia GS *et al.* Hypoxia-inducible factor-2 alpha up-regulates CD70 under hypoxia and enhances anchorage-independent growth and aggressiveness in cancer cells. *Oncotarget* 2018; **9**: 19123–19135.

42 Riether C, Schurch CM, Flury C, Hinterbrandner M, Druck L, Huguenin A-L *et al.* Tyrosine kinase inhibitor-induced CD70 expression mediates drug resistance in leukemia stem cells by activating Wnt signaling. *Sci Transl Med* 2015; **7**: 298ra119-298ra119.

43 Hugo W, Zaretsky JM, Sun L, Song C, Moreno BH, Hu-Lieskovan S *et al.* Genomic and Transcriptomic Features of Response to Anti-PD-1 Therapy in Metastatic Melanoma. *Cell* 2016. doi:10.1016/j.cell.2016.02.065.

44 Chae YK, Chang S, Ko T, Anker J, Agte S, Iams W *et al.* Epithelial-mesenchymal transition (EMT) signature is inversely associated with T-cell infiltration in non-small cell lung cancer (NSCLC). *Sci Rep* 2018; **8**: 2918.

45 Tauriello DVF, Palomo-Ponce S, Stork D, Berenguer-Llergo A, Badia-Ramentol J, Iglesias M *et al.* TGFβ drives immune evasion in genetically reconstituted colon cancer metastasis. *Nature* 2018; **554**: 538–543.

46 Claus C, Riether C, Schürch C, Matter MS, Hilmenyuk T, Ochsenbein AF. CD27 signaling increases the frequency of regulatory T cells and promotes tumor growth. *Cancer Res* 2012; **72**: 3664–3676.

47 Yang ZZ, Novak AJ, Ziesmer SC, Witzig TE, Ansell SM. CD70+ non-Hodgkin lymphoma B cells induce Foxp3 expression and regulatory function in intratumoral CD4+CD25- T cells. *Blood* 2007; **110**: 2537–2544.

48 Kargl J, Busch SE, Yang GHY, Kim KH, Hanke ML, Metz HE *et al.* Neutrophils dominate the immune cell composition in non-small cell lung cancer. *Nat Commun* 2017; **8**: 1–11.

49 Hedrick CC, Malanchi I. Neutrophils in cancer: heterogeneous and multifaceted. Nat. Rev. Immunol. 2021; **22**: 173–187.

50 Faget J, Groeneveld S, Boivin G, Sankar M, Zangger N, Garcia M *et al.* Neutrophils and Snail Orchestrate the Establishment of a Pro-tumor Microenvironment in Lung Cancer. *Cell Rep* 2017; **21**: 3190–3204.

51 Singhal S, Bhojnagarwala PS, O'Brien S, Moon EK, Garfall AL, Rao AS *et al.* Origin and Role of a Subset of Tumor-Associated Neutrophils with Antigen-Presenting Cell Features in Early-Stage Human Lung Cancer. *Cancer Cell* 2016; **30**: 120–135.

52 Al Sayed MF, Ruckstuhl CA, Hilmenyuk T, Claus C, Bourquin JP, Bornhauser BC *et al.* CD70 reverse signaling enhances NK cell function and immunosurveillance in CD27-expressing B-cell malignancies. *Blood* 2017; **130**: 297–309.

53 Riether C, Schürch CM, Flury C, Hinterbrandner M, Drück L, Huguenin AL *et al.* Tyrosine kinase inhibitor-induced CD70 expression mediates drug resistance in leukemia stem cells by activating Wnt signaling. *Sci Transl Med* 2015; **7**. doi:10.1126/scitranslmed.aab1740.

54 Chahlavi A, Rayman P, Richmond AL, Biswas K, Zhang R, Vogelbaum M *et al.* Glioblastomas induce T-lymphocyte death by two distinct pathways involving gangliosides and CD70. *Cancer Res* 2005; **65**: 5428–5438.

55 Diegmann J, Junker K, Loncarevic IF, Michel S, Schimmel B, von Eggeling F. Immune escape for renal cell carcinoma: CD70 mediates apoptosis in lymphocytes. *Neoplasia* 2006; **8**: 933–938.

56 Jak M, Mous R, Remmerswaal EBM, Spijker R, Jaspers A, Yagüe A *et al.* Enhanced formation and survival of CD4+ CD25hi Foxp3+ T-cells in chronic lymphocytic leukemia. *Leuk Lymphoma* 2009; **50**: 788–801.

57 Yang Z-Z, Grote DM, Xiu B, Ziesmer SC, Price-Troska TL, Hodge LS *et al.* TGF-β upregulates CD70 expression and induces exhaustion of effector memory T cells in B-cell non-Hodgkin's lymphoma. *Leukemia* 2014; **28**: 1872–1884.

58 Tesselaar K, Arens R, van Schijndel GMW, Baars PA, van der Valk MA, Borst J *et al.* Lethal T cell immunodeficiency induced by chronic costimulation via CD27-CD70 interactions. Nat. Immunol. 2003; **4**: 49–54.

59 Winkels H, Meiler S, Lievens D, Engel D, Spitz C, Bürger C *et al.* CD27 co-stimulation increases the abundance of regulatory T cells and reduces atherosclerosis in hyperlipidaemic mice. *Eur Heart J* 2017; **38**: 3590–3599.

60 Coquet JM, Ribot JC, Bąbala N, Middendorp S, van der Horst G, Xiao Y *et al.* Epithelial and dendritic cells in the thymic medulla promote cd4+foxp3+ regulatory t cell development via the cd27-cd70 pathway. *J Exp Med* 2013; **210**: 715–728.

61 Jacobs J, Zwaenepoel K, Rolfo C, Van den Bossche J, Deben C, Silence K *et al.* Unlocking the potential of CD70 as a novel immunotherapeutic target for non-small cell lung cancer. *Oncotarget* 2015; **6**: 13462–75.

62 Aftimos P, Rolfo C, Rottey S, Offner F, Bron D, Maerevoet M *et al.* Phase I dose-escalation study of the anti-CD70 antibody ARGX-110 in advanced malignancies. *Clin Cancer Res* 2017; **23**: 6411–6420.

63 Riether C, Pabst T, Höpner S, Bacher U, Hinterbrandner M, Banz Y *et al.* Targeting CD70 with cusatuzumab eliminates acute myeloid leukemia stem cells in patients treated with hypomethylating agents. *Nat Med* 2020; **26**: 1459–1467.

64 Weissferdt A, Kalhor N, Canales JR, Fujimoto J, Wistuba II, Moran CA. Spindle cell and pleomorphic ("sarcomatoid") carcinomas of the lung: an immunohistochemical analysis of 86 cases. *Hum Pathol* 2016. doi:10.1016/j.humpath.2016.08.003.

65 Bae H-M, Min HS, Lee S-H, Kim D-W, Chung DH, Lee J-S *et al.* Palliative chemotherapy for pulmonary pleomorphic carcinoma. *Lung Cancer* 2007; **58**: 112–115.

66 Vieira T, Girard N, Ung M, Monnet I, Cazes A, Bonnette P *et al.* Efficacy of First-Line Chemotherapy in Patients with Advanced Lung Sarcomatoid Carcinoma. 2013 doi:10.1097/01.JTO.0000437008.00554.90.

67 Manzotti G, Torricelli F, Benedetta D, Lococo F, Sancisi V, Rossi G *et al.* An epithelial-to-mesenchymal transcriptional switch triggers evolution of pulmonary sarcomatoid carcinoma (PSC) and identifies dasatinib as new therapeutic option. *Clin Cancer Res* 2019; **25**: 2348–2360.

68 Domblides C, Leroy K, Monnet I, Mazières J, Barlesi F, Gounant V *et al.* Efficacy of Immune Checkpoint Inhibitors in Lung Sarcomatoid Carcinoma. *J Thorac Oncol* 2020; **15**: 860–866.

69 Lococo F, Gandolfi G, Rossi G, Pinto C, Rapicetta C, Cavazza A *et al.* Deep sequencing analysis reveals that KRAS mutation is a marker of poor prognosis in patients with pulmonary sarcomatoid carcinoma. *J Thorac Oncol* 2016; **11**: 1282–1292.

70 Awada A, Rolfo CD, Rottey S, Ysebrant de Lendonck L, Schroyens WA, Offner F *et al.* A phase I, first-in-human study of ARGX-110, a monoclonal antibody targeting CD70, a receptor involved in immune escape and tumor growth in patients with solid and hematologic malignancies. *J Clin Oncol* 2014; **32**: 3023–3023.

71 Leupin N, Zinzani PL, Morschhauser F, Dalle S, Maerevoet M, Michot JM *et al.* Cusatuzumab for treatment of CD70-positive relapsed or refractory cutaneous T-cell lymphoma. *Cancer* 2021; **128**: 1004–1014.

72 Becht E, Giraldo NA, Lacroix L, Buttard B, Elarouci N, Petitprez F *et al.* Estimating the?population abundance of tissue-infiltrating immune and stromal cell populations using gene expression. *Genome Biol* 2016; **17**: 218.

FIGURE LEGENDS

Figure 1. *CD70* expression is associated with a mesenchymal status in NSCLC cell lines. A) Unsupervised clustering of ICPL expression in 130 NSCLC cell lines from the CCLE according to the EMT pan-cancer score[11]. EMT pan-cancer status, E (pink) or M (blue). EMT pan-cancer score, low (yellow) or high (red). B) *CD70* gene expression between epithelial and mesenchymal NSCLC cell lines from the CCLE. Significance was determined with Mann–Whitney U test. C) Protein expression of ZEB1, E-cadherin, Vimentin, SNAIL, TWIST1 and alpha-tubulin in two epithelial (H3255 and H441) and two mesenchymal (HCC44 and H23) NSCLC cell lines. Whole-cell lysates were analyzed by immunoblotting. Graphical representation (D) and quantification (E) of the expression levels of CD70, as expressed in median fluorescent intensity (MFI) values, in selected NSCLC cell lines, evaluated by flow cytometry. Data are represented as mean ± s.d. (n=3 independent experiments). Significance was determined using an unpaired *t* test. * $P < 0.05$; ** $P < 0.01$; *** $P < 0.001$.

Figure 2. *In vitro* modulation of ZEB1 impacts CD70 expression. A. Assessment of EMT-pancancer signature score[11] in CDK4/TERT-immortalized human bronchial epithelial cells (HBECs) stably transduced with a pMSCV-ZEB1 retroviral vector[26]. Top differentially expressed genes between HBEC3^{pMSCV} and HBEC3^{ZEB1} cells (B, left panel) and graphical representation of *CD70* expression in HBEC3^{pMSCV} and HBEC3^{ZEB1} cells (B, right panel). C. Immunoblot analyses of ZEB1, E-cadherin and tubulin in HCC44 cells that underwent a CRISPR/Cas9-mediated ZEB1 knockout (sg: guide RNA, sgCtrl: control). D. Graphical representation and quantification of CD70 expression, as evaluated by flow cytometry, expressed in median fluorescent intensity (MFI) values, in HCC44 control (sgCtrl) and HCC44-ZEB1 knockout cell lines (sgZEB1 #1 to #3). Data are represented as mean ± s.d. (n=3 independent experiments). E. *ZEB1* expression as assessed by qRT-PCR (left) and immunoblot analyses (right) for ZEB1 and vimentin in ZEB1-expressing PC9 cells compared to control (e.v.: empty vector). Plasmid expression (e.v or ZEB1) was induced by doxycyclin treatment. qRT-PCR values are the

average of biologic duplicates from three independent experiments. F. *CD70* promoter activity, as assessed by a Gaussia luciferase assay, in ZEB1 expressing cells when compared to control (e.v). The relative Gaussia luciferase activity was normalized against the activity of secreted alkaline phosphatase (SeAP). Data are represented as mean ± s.d. (n=2 independent experiments). G. *CD70* expression as assessed by qRT-PCR in ZEB1 expressing PC9 cells compared to control (e.v). Values are the average of biologic duplicates from two experiments. Significance was determined using an unpaired *t* test. * $P < 0.05$; ** $P < 0.01$.

Figure 3. Impact of CD70 inhibition in mesenchymal lung cancer preclinical models. A. Immunoblot to assess the protein expression of CD70, EMT-transcription factors and effectors of apoptosis in HCC44 and H23 cells transfected with a siRNA targeting CD70 (siCD70) or a control siRNA (siCtrl) for 96 hours. B. Histogram of ssGSEA enrichment analysis of the biological pathways significantly affected in HCC44 cells upon CD70 knock-down.

Figure 4. Mesenchymal NSCLC tumors expressed increased *CD70* mRNA levels. Gene expression levels of *CD70* according to the EMT status[11] in A. lung adenocarcinomas (ADC, n=517), B. lung squamous cell carcinomas (SqCC, n=501) from the TCGA dataset and in C. lung ADC (n=80), lung SqCC (n=80) and pulmonary sarcomatoid carcinomas (n=4) from the GSE41271 dataset. D. *CD70* expression in lung tumor tissue versus in comparison to normal lung samples, in three independent datasets. **** $P < 0.0001$; NS, not significant.

Figure 5. Pulmonary sarcomatoid carcinomas exhibit high ZEB1 expression and are enriched for CD70 expression. A. Immunohistochemical staining of ZEB1, as assessed by the percentage of positive cells, of full tumor sections of 52 ADC and 47 SqCC and 55 pulmonary SC. B. Transcriptional EMT pancancer signature score in 51 ADC, 44 SqCC and 40 pulmonary SC. Targeted transcriptome sequencing was performed using the HTG-EdgeSeq technology. C. Spearman correlation of the transcriptional EMT pancancer signature and the mRNA expression levels of EMT-related transcription factors and *CDH1* (E-cadherin). D.

Immunohistochemical staining of CD70 in full tumor sections of 52 ADC and 47 SqCC and 55 pulmonary SC. The median value (*H*-score=100) was used to define the low and high CD70 expression groups. Scale bar represents 200µM. E. Transcriptional EMT pancancer signature score of paired epithelial (E) and spindle-cells (SP) compartments of 11 pleomorphic pulmonary SC (Wilcoxon matched-pairs signed rank test, ** $P < 0.001$). Visual quantification of immunostaining for ZEB1 (F) and CD70 (G) in the epithelial (E) and spindle-cell (SP) compartments of 11 pleomorphic pulmonary SC (Wilcoxon matched-pairs signed rank test, ** $P < 0.001$). The scale bar represents 300µM.

Figure 6. Decreased tumor-infiltrating CD3$^+$ T cells and CD8$^+$ T cells in pulmonary sarcomatoid carcinomas expressing high levels of CD70. Automated quantification, as assessed by the number of positive cells per mm^2, of the immunohistochemical staining of CD3 (A) and CD8 (C) positive T-cells in pulmonary SC (n=55). Representative images of the immunostaining are presented in C. Spearman correlation of *CD70* mRNA expression levels and (D) markers of T cell exhaustion (*i.e., HAVCR2, LAG3 and PDCD1*) and (E) *FOXP3*, a marker of regulatory T cells, in 51 ADC, 44 SqCC and 40 pulmonary sarcomatoid carcinomas. F. Deconvolution of immune infiltrate between CD70^{LOW} and CD70^{HIGH} sarcomatoid carcinomas, using MCPcounter[72] (Wilcoxon test).

Figure 1

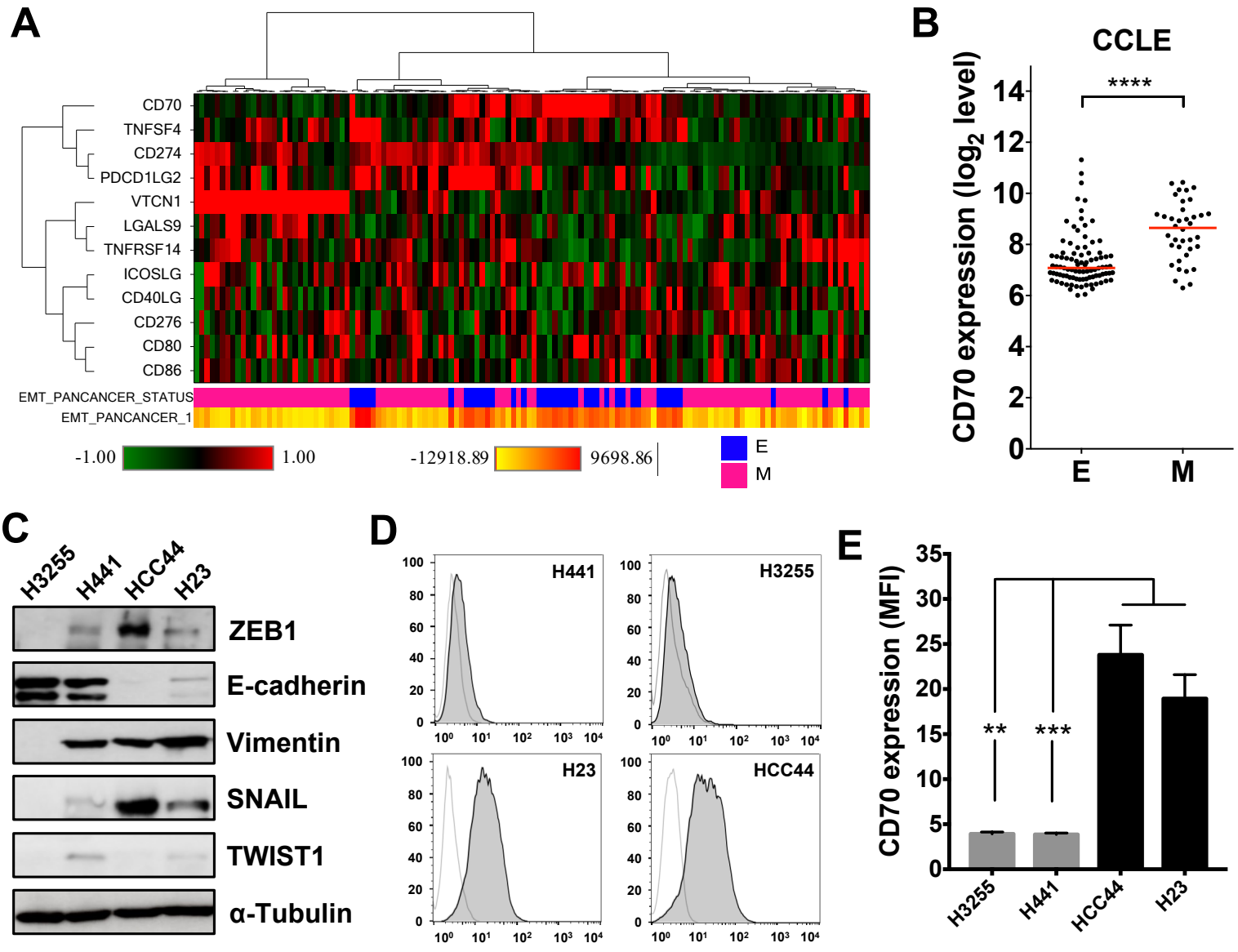
A
CD70
TNFSF4
CD274
PDCD1LG2
VTCN1
LGALS9
TNFRSF14
ICOSLG
CD40LG
CD276
CD80
CD86
EMT_PANCANCER_STATUS
EMT_PANCANCER_1
-1.00
1.00
-12918.89
9698.86
E
M
B
CCLE
****
CD70 expression (log2 level)
E
M
C
H3255
H441
HCC44
H23
ZEB1
E-cadherin
Vimentin
SNAIL
TWIST1
α-Tubulin
D
H441
H3255
H23
HCC44
E
CD70 expression (MFI)
**
***
H3255
H441
HCC44
H23

Figure 2

A

GEO ID	Sample name	Score EMT_MAK	Status
GSM2061439	HBEC3 pMSCV	-9240,15	E
GSM2061441	HBEC3 ZEB1.1	-734,15	M

B

Gene name	HBEC3 ZEB1	HBEC3 pMSCV	(HBEC3_ZEB1) - (HBEC3_pMSCV)
CPA4	11.161	2.104	9.057
HCFC1	9.91	1	8.91
ALDH3A1	10.73	2.868	7.862
S100A8	11.241	3.907	7.334
VCAN	10.577	3.472	7.105
GAS1	9.7245	2.677	7.0475
CA9	9.113	2.35	6.763
IGFBP2	12.086	5.466	6.62
CD70	9.88	3.818	6.062
HSPA8	11.3865	5.4665	5.92

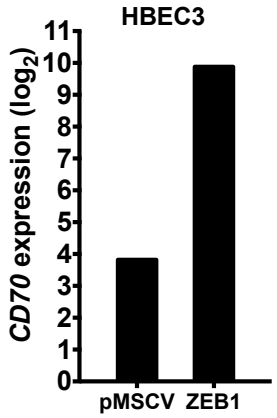

C

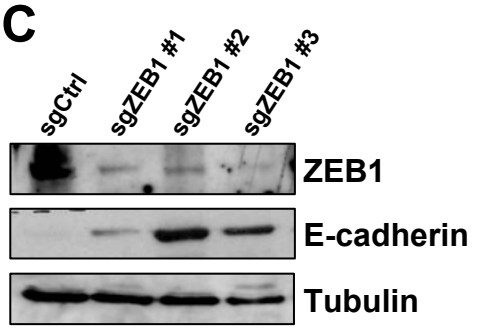

D

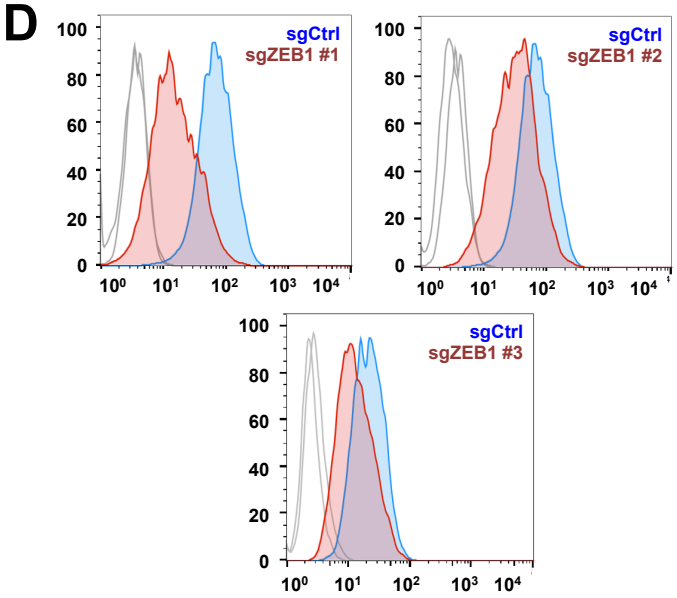

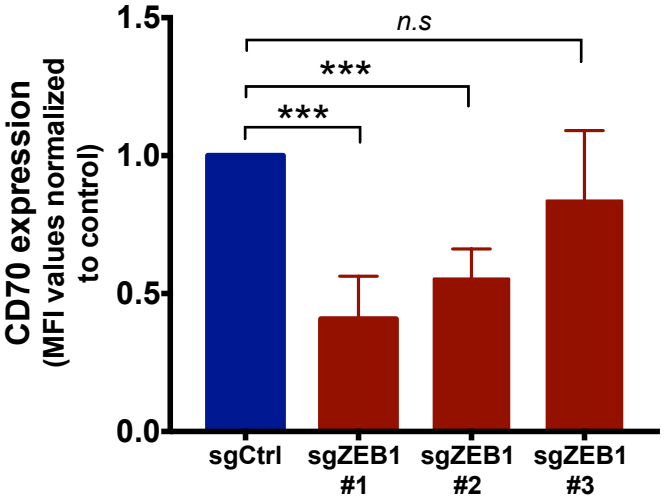

E

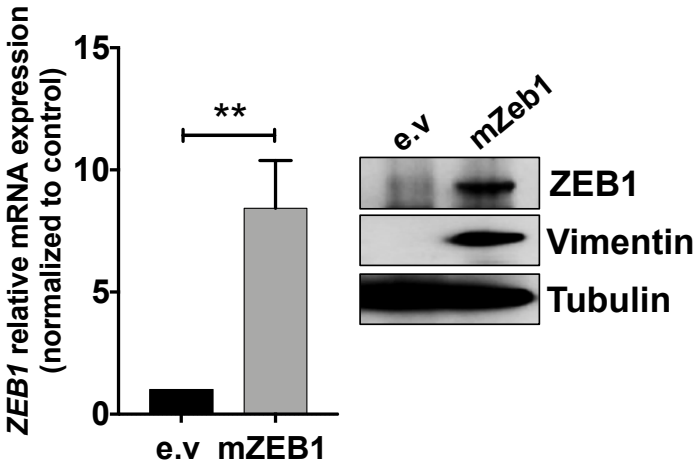

F

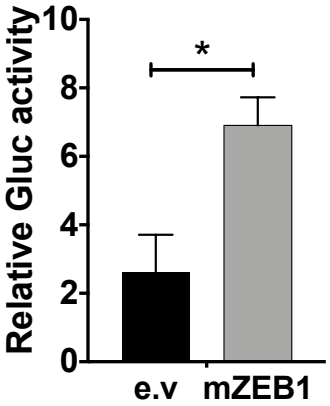

G

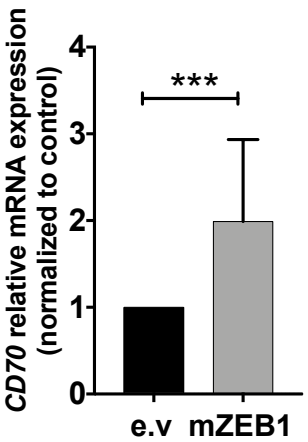

Figure 3

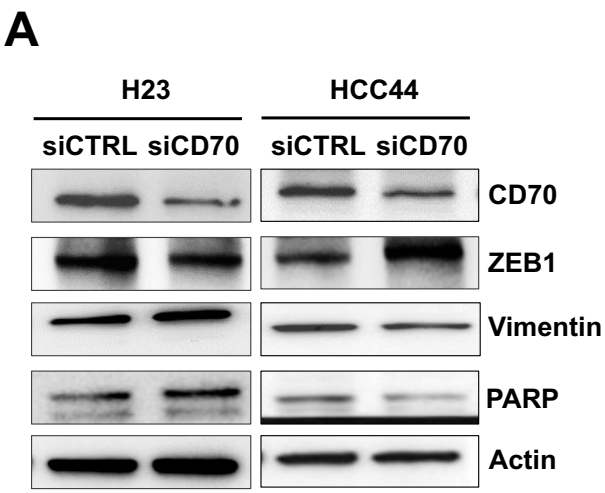
A
H23
HCC44
siCTRL siCD70
siCTRL siCD70
CD70
ZEB1
Vimentin
PARP
Actin

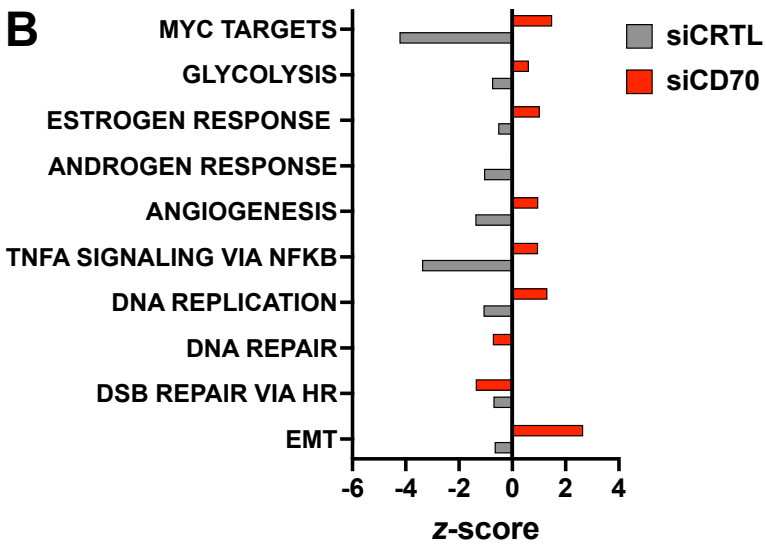
B
MYC TARGETS
GLYCOLYSIS
ESTROGEN RESPONSE
ANDROGEN RESPONSE
ANGIOGENESIS
TNFA SIGNALING VIA NFKB
DNA REPLICATION
DNA REPAIR
DSB REPAIR VIA HR
EMT
-6
-4
-2
0
2
4
z-score
siCRTL
siCD70

Figure 4

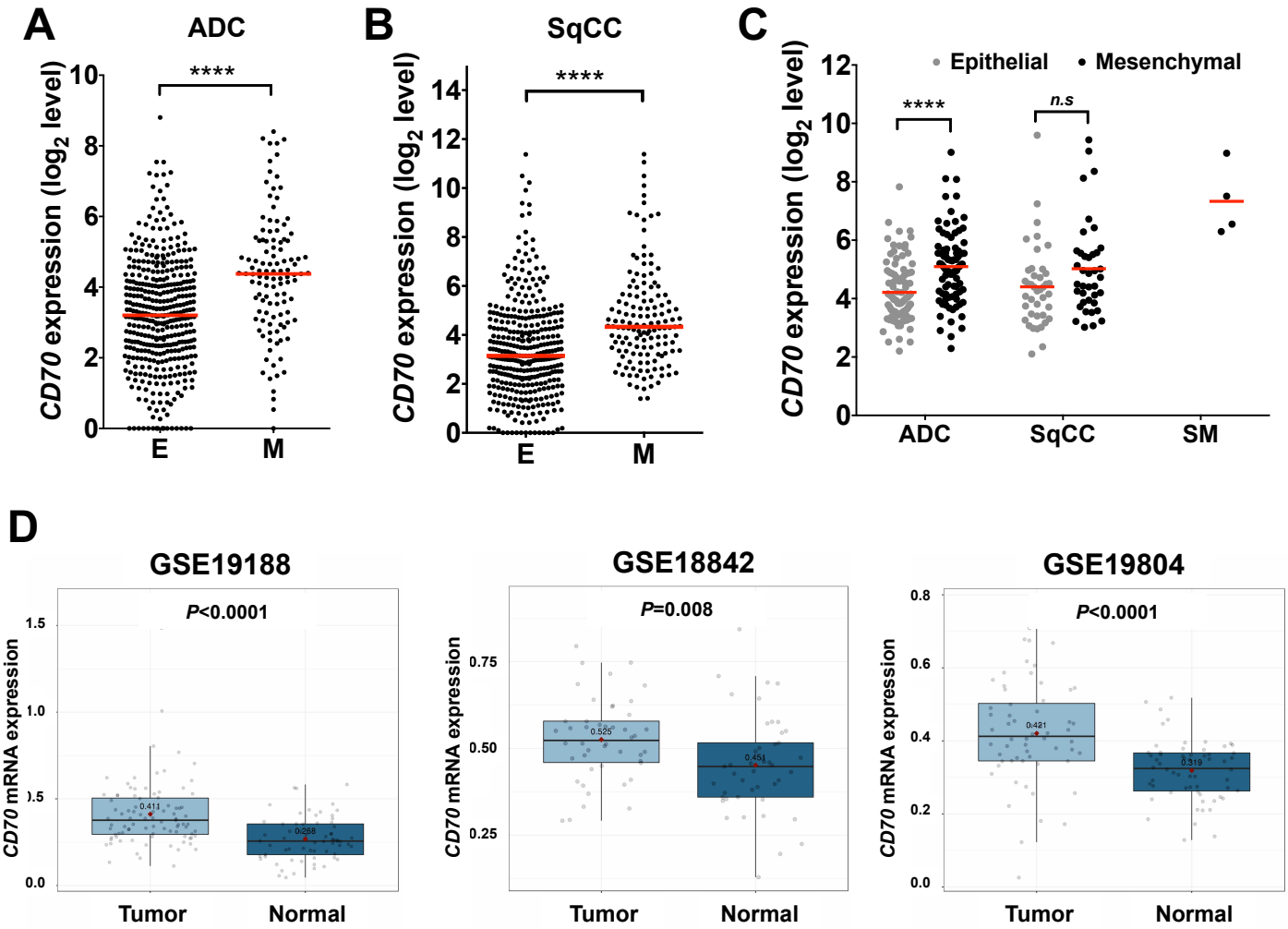
A
ADC
****
CD70 expression (log2 level)
E
M
B
SqCC
****
CD70 expression (log2 level)
E
M
C
Epithelial
Mesenchymal
****
n.s
CD70 expression (log2 level)
ADC
SqCC
SM
D
GSE19188
P<0.0001
CD70 mRNA expression
Tumor
Normal
GSE18842
P=0.008
CD70 mRNA expression
Tumor
Normal
GSE19804
P<0.0001
CD70 mRNA expression
Tumor
Normal

Figure 5

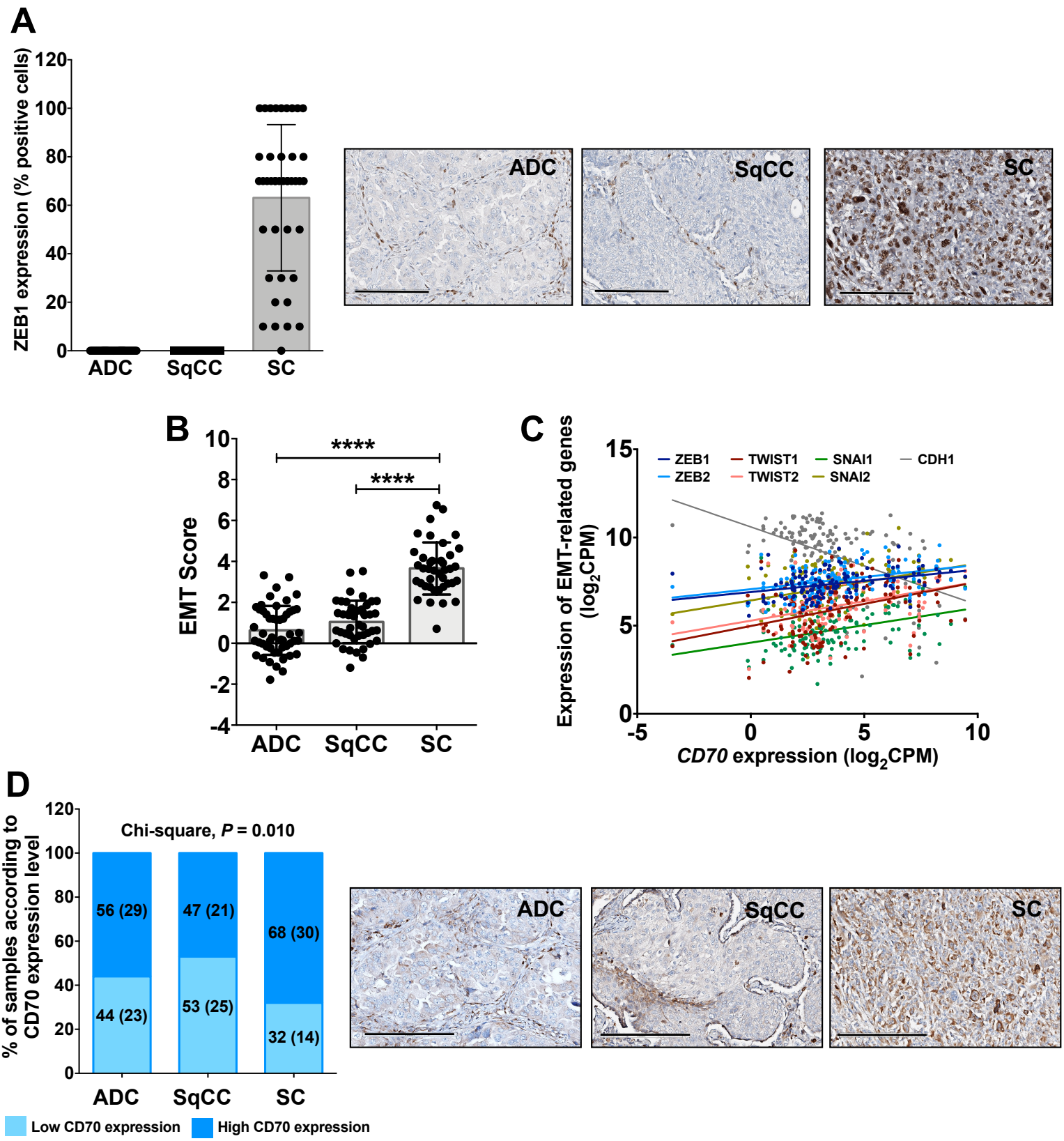
A
ZEB1 expression (% positive cells)
120
100
80
60
40
20
0
ADC
SqCC
SC
ADC
SqCC
SC
B
EMT Score
10
8
6
4
2
0
-2
-4
****
****
ADC
SqCC
SC
C
Expression of EMT-related genes (log2CPM)
15
10
5
0
-5
0
5
10
CD70 expression (log2CPM)
ZEB1
ZEB2
TWIST1
TWIST2
SNAI1
SNAI2
CDH1
D
% of samples according to CD70 expression level
120
100
80
60
40
20
0
Chi-square, P = 0.010
56 (29)
44 (23)
47 (21)
53 (25)
68 (30)
32 (14)
ADC
SqCC
SC
Low CD70 expression
High CD70 expression
ADC
SqCC
SC

Figure 5 - continued

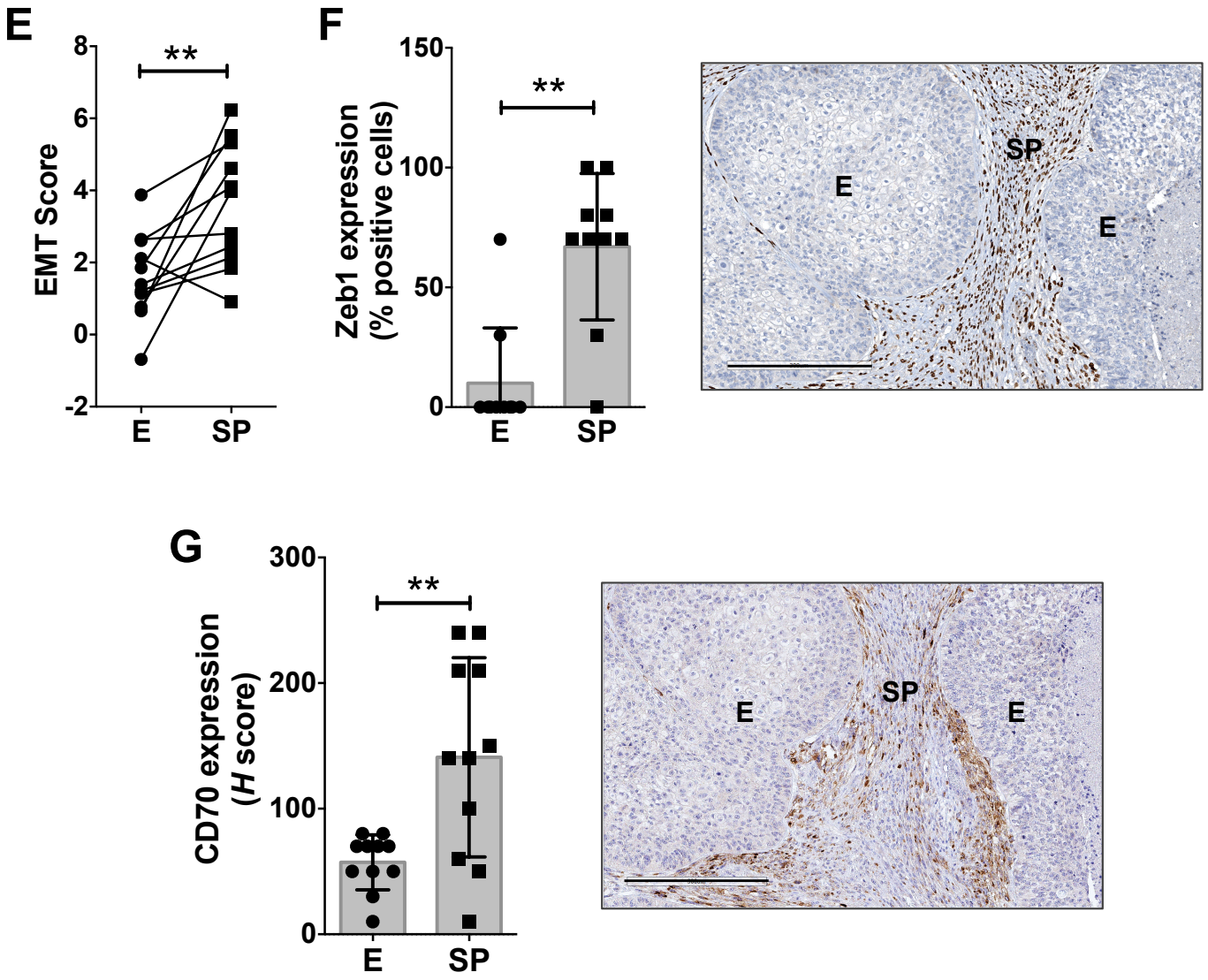

Figure 6

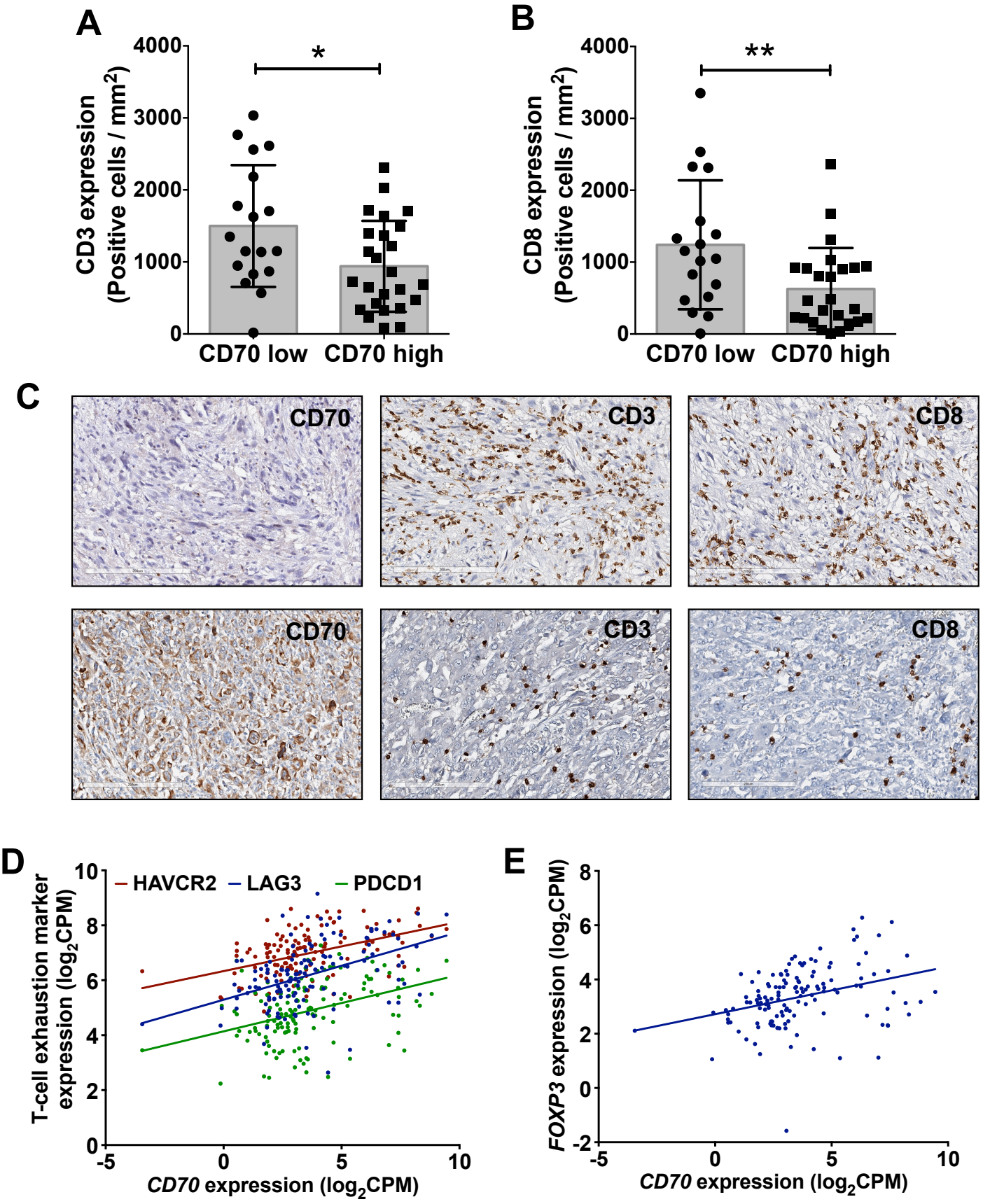
A
CD3 expression (Positive cells / mm2)
4000
3000
2000
1000
0
*
CD70 low
CD70 high
B
CD8 expression (Positive cells / mm2)
4000
3000
2000
1000
0
**
CD70 low
CD70 high
C
CD70
CD3
CD8
CD70
CD3
CD8
D
HAVCR2
LAG3
PDCD1
T-cell exhaustion marker expression (log2CPM)
10
8
6
4
2
0
-5
0
5
10
CD70 expression (log2CPM)
E
FOXP3 expression (log2CPM)
8
6
4
2
0
-2
-5
0
5
10
CD70 expression (log2CPM)

Figure 6 - continued

F

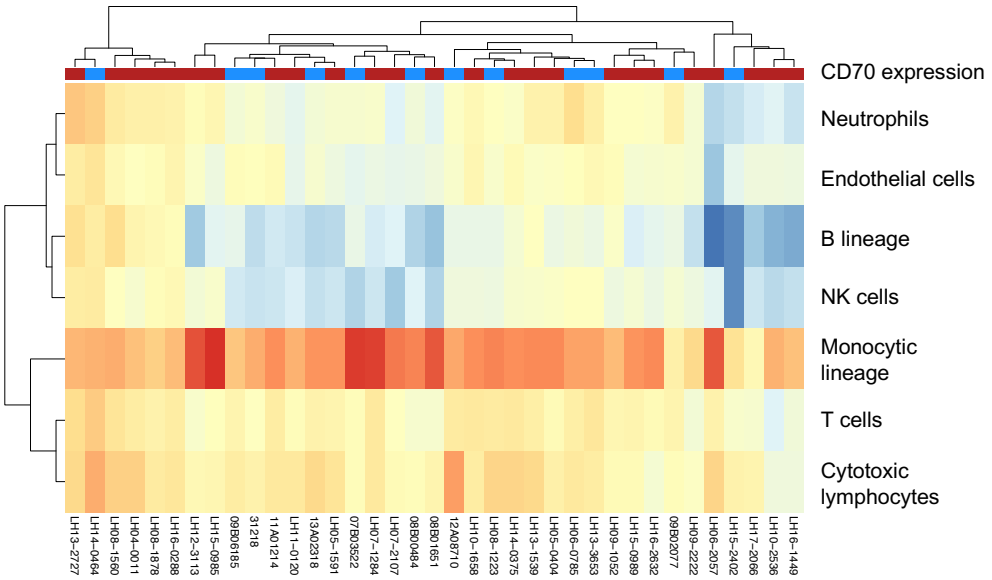

Cell population	Estimate	Pr(>|z|)
B lineage	1,696	0,072
Cytotoxic lymphocytes	-1,319	0,229
Endothelial cells	0,558	0,690
Monocytic lineage	1,343	0,068
Neutrophils	-5,348	0,015
NK cells	3,631	0,023
T cells	-0,362	0,829